QUALIFYING AL-800 GARNET FOR THE FERMILAB BOOSTER PERPENDICULAR BIASED 2ND HARMONIC RF CAVITY

John C. Kuharik

Submitted to the faculty of the University Graduate School

in partial fulfillment of the requirement

for the degree

Master of Science

in the Department of Physics,

Indiana University

June, 2021

Accepted by the Graduate Faculty, Indiana University, in partial fulfillment of the requirement for the degree of Master of Science.

Master's Thesis Committee

William Michael Snow, Ph.D.

Joshua C. Long, Ph.D.

Cheng-Yeng Tan, Ph.D.

Robyn Madrak, Ph.D.

Acknowledgments

A number of people have provided support and assistance during the completion of this thesis. I would like to thank my primary advisors Cheng-Yang Tan and Robyn Madrak for their guidance and patience throughout this long process. I would like to acknowledge my thesis defense committee members Dr. Mike Snow and Dr. Joshua Long. I would like to thank Susan Winchester, Irina Novitski, Bill Barletta, Steven Lund, and everyone involved in the USPAS program for their ongoing effort to make such a wonderful program possible. I would like to thank Dan Johnson and Salah Chaurize for allowing me to participate in the USPAS program. I would also like to thank the Iouri Terechkine for his guidance and consultation, Tyler Fronk for his reliable partnership and support during USPAS sessions, Chris Olsen for his assistance in all things mechanical, Adam Watts for introducing me to Python and providing me with good advice, and Todd Johnson for lending me some of his devices.

Finally, I would like to express my eternal gratitude to my beautiful wife Lindy for her unlimited patience and support. Without her, none of this would have been possible.

This document was prepared using the resources of the Fermi National Accelerator Laboratory (Fermilab), a U.S. Department of Energy, Office of Science, HEP User Facility. Fermilab is managed by Fermi Research Alliance, LLC (FRA), acting under Contract No. DE-AC02-07CH11359.

John C. Kuharik

Qualifying AL-800 Garnet for the Fermilab Booster Perpendicular Biased 2nd Harmonic RF Cavity

Al-800 garnet was evaluated for the perpendicular biased 2nd harmonic cavity for the Fermilab Booster accelerator. A test apparatus was designed to evaluate the magnetic permeability and batch consistency of small witness samples of Al-800. Fully assembled AL-800 garnet rings were tested on the garnet ring test stand to measure the resonant frequency and quality factor of each ring. The garnet witness samples and assembled garnet rings showed acceptable consistency within the parameters set by the cavity design team. Based on the test results, AL-800 garnet was deemed suitable for use in the perpendicular biased 2nd harmonic cavity.

Contents

List of Tables

List of Figures

Chapter 1

Introduction

The Booster accelerator at Fermilab is a rapid cycling synchrotron that has been operating since 1971. Originally designed as a 200 MeV to 8 GeV accelerator, it has undergone many upgrades and now accepts 400 MeV H- ions from the Linac accelerator and delivers 8 GeV protons at 15 Hz to the Main Injector, Recycler, and the Booster Neutrino Beamline [1]. As Fermilab pushes the intensity frontier towards a 1 MW neutrino production beam, demands on the Booster have increased. More beam intensity is desired at a greater efficiency than is currently provided. A late addition to Fermilab's Proton Improvement Plan [2] is the development and installation of a perpendicular biased 2nd harmonic RF cavity for the Booster [3].

Figure 1.1 shows the design schematic for the 2nd harmonic cavity and Figure 1.2 shows the assembled cavity prior to installation. This design will allow for increased capture efficiency at injection, a smoother transition crossing, and greater control during bunch rotation during extraction [4]. This is achieved by flattening the RF bucket which increases the stable phase space available to the beam particles [5]. A perpendicular biased cavity was chosen for the final design so that a single cavity would be able to achieve the stated goals. The cavity was designed to be tunable across a wide frequency range, and to have a high quality factor, or Q.

The main accelerating cavities in the Booster are parallel biased cavities with a frequency swing from 37.77 MHz to 52.81 MHz. The 2nd harmonic cavity will be perpendicular biased and have a frequency range twice the fundamental frequency from 75.73 MHz to 105.63 MHz. Compared to a parallel bias field, a perpendicular bias allows for a higher Q because in this scheme the material is biased to near saturation. The available ferrite materials such as the NiZn ferrite ($NiZnFe_2O_4$),

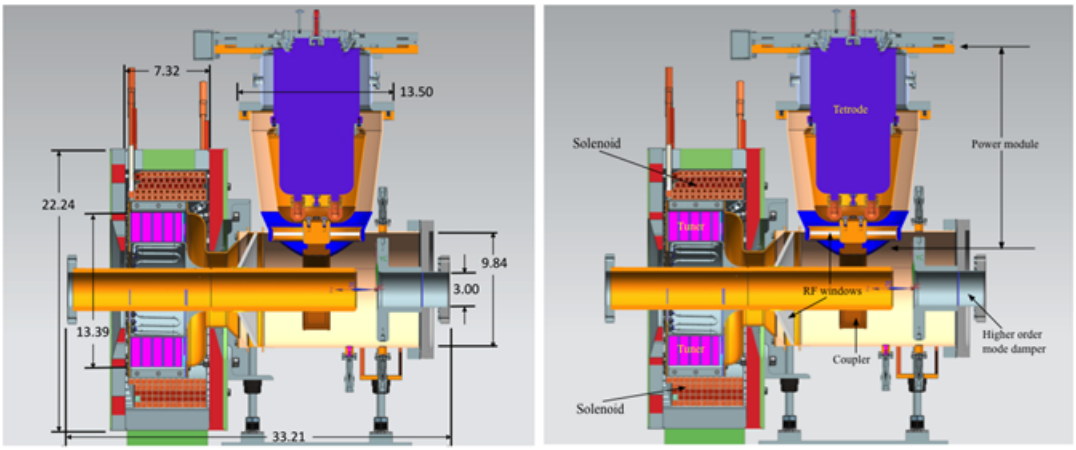

Figure 1.1: Cross-sectional diagram of the 2nd harmonic cavity design.

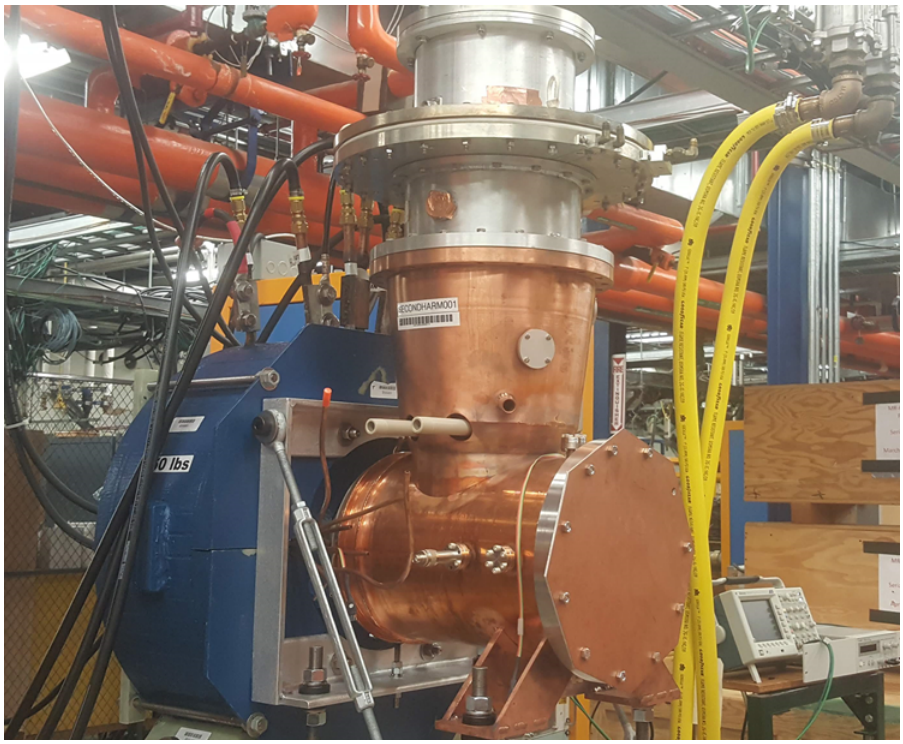

Figure 1.2: Photo of the assembled 2nd harmonic cavity.

currently in use in the Booster parallel biased cavities, have a saturation magnetization that is prohibitively large (3.2 kG) for operation near saturation [6]. Garnet ferrites ($Y_3Fe_5O_{12}$), in general, have a lower saturation magnetization than NiZn ferrite and the saturation properties of garnet ferrite can also be lowered by doping with aluminum [7]. As an aluminum doped garnet, AL-800 saturates at a much lower bias field near 800 G, and so it is more suited for the perpendicular bias scheme in the 2nd harmonic cavity [8, 9]. Materials with lower saturation are available, however they also have a lower Curie point. For example, AL-400 saturates at 400 G and has a Curie point of 130°C, whereas the AL-800 Curie point is 200°C, which is well above the 2nd harmonic cavity design operational temperature of less than 100°C [8].

The 2nd harmonic cavity bias tuner design, shown in Figure 1.3, consists of a solenoid around six alumina backed AL-800 rings with an outer diameter of 340 mm. The rings are within the cavity resonant structure, and their permeability changes with the applied bias field from the solenoid. Local variations of the complex permeability can cause RF loss and temperature hot spots that could damage the rings [10]. One source of variation in permeability across the tuner stack are the areas of nonuniform bias field in the tuner. To address one such area, the tuner stack was designed with a specially shaped AL-800 shim ring. The shim ring helps shape the bias field at the interface of the loaded and unloaded cavity areas. Another possible source of permeability variation is the variation of magnetic properties within the tuner stack and within each ring. It is important that the garnet rings all have the same magnetic properties, however, it is expected that the permeability will have some variation across the bias tuner due to manufacturing imperfections and because of the cooling rings.

National Magnetics is currently the only manufacturer of large AL-800 garnet. Due to the equipment limitations, the AL-800 garnet rings could not be made as a single unit of AL-800 material. The size of the manufacturer's oven used to prepare the material required that the rings be assembled from eight separately prepared sectors, epoxied together to form each ring. The possibility of variation between manufacturing batches made it necessary to test each batch for consistency. The manufacturer provided witness samples from each portion of the batches that were used to create the garnet ring sectors. The permeability of the witness samples was measured in a test stand built for that purpose, and the performance of the assembled rings was tested

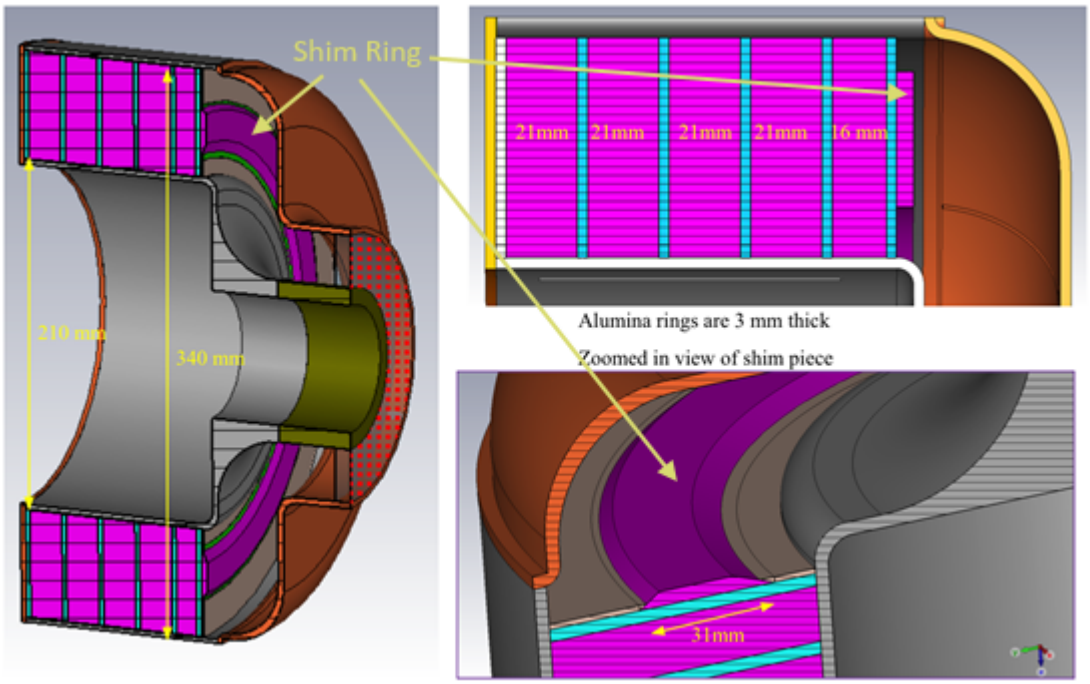

Figure 1.3: The 2nd harmonic cavity bias tuner design. The garnet rings (magenta) are each backed by an 3 mm alumina ring (cyan).

in a specially designed RF cavity. This thesis details the development of the test methods and the test results characterizing the AL-800 garnet witness samples and assembled garnet rings.

Chapter 2

AL-800 Witness Sample Testing

The garnet rings specified for the 2nd harmonic cavity bias tuner are made from eight separate pieces epoxied together. Because of this, it is imperative that the magnetic properties of the garnet are as consistent as possible between manufacturing batches. Inconsistent permeability of the different garnet sectors could cause uneven deposition of RF energy and significant heating in the garnet during cavity operation, and result in damage to the bias tuner [10]. Figure 2.1 shows the relative sizes of the manufactured garnet block and the garnet ring sectors cut from each block. Witness samples corresponding to each sector were cut from the same block.

Measurement of the garnet batch consistency was done in two steps. First, witness samples corresponding to each ring sector piece were measured in the garnet witness piece test stand designed by I. Terechkine (FNAL). Modifications to the test stand by the author will be discussed in section 2.2. Second, the fully assembled garnet rings were tested in the garnet ring test stand designed by I. Terechkine, A. Makarov, and G. Romanov (FNAL), with further modifications as described by the author. The garnet witness piece test stand was used to measure the real part of permeability of the witness pieces. The witness pieces are small cylindrical samples cut from the rectangular blocks that were used to manufacture each sector of the garnet ring. Each garnet sector and its corresponding witness piece are paired by their identification numbers.

The goal for testing the garnet witness samples was to determine whether the magnetic permeability of the samples is near the specification value provided by the manufacturer and whether all the samples have the same permeability within 5%.

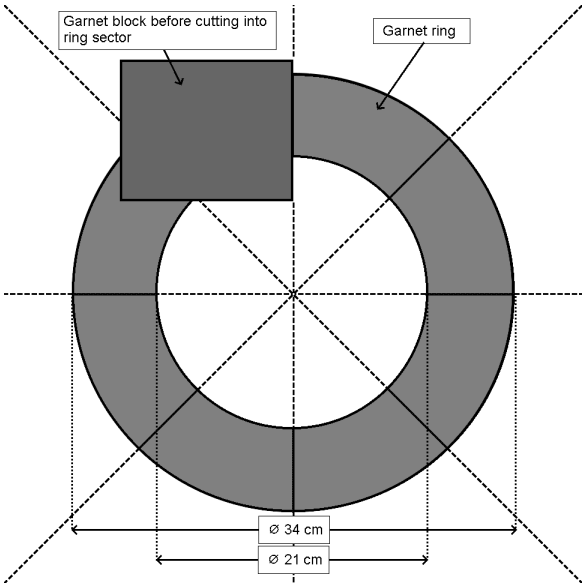

Figure 2.1: The eight garnet ring sectors were cut from rectangular garnet blocks. Witness samples corresponding to each sector were cut from the same block.

2.1 Witness Sample Testing Theory

In free space, the magnetic flux density $\boldsymbol{B}$ is related to the magnetic field strength $\boldsymbol{H}$ by the permeability of free space μ_0, i.e.

$$\boldsymbol{B} = \mu_0 \boldsymbol{H} \tag{2.1.1}$$

where $\boldsymbol{B}$ is the magnetic flux density in Teslas, $\boldsymbol{H}$ is the applied magnetic field strength in amperes per meter and $\mu_0 = 4\pi \times 10^{-7}$ H/m is the permeability of free space.

In a magnetic material, such as the AL-800 garnet,

$$\boldsymbol{B_M} = \mu_r \mu_0 \boldsymbol{H_M} \tag{2.1.2}$$

where μ_r is the relative permeability of the material, $\boldsymbol{B_M}$ and $\boldsymbol{H_M}$ are the magnetic flux density and field strength within the material, respectively.

Equation 2.1.2 forms the basis for extracting μ_r once the magnetic field strength, $\boldsymbol{H_M}$, is known. In the setup shown in Figure 2.2, a known current, I, is applied to an excitation coil which surrounds the sample. The voltage induced in the measurement coil is then measured.

Using Ampere's Law, the closed path line integral, shown in red in the figure, is

$$\oint \boldsymbol{H_M} \cdot d\boldsymbol{l} = N_e I \tag{2.1.3}$$

where N_e is the number of turns in the excitation coil. If the integration path is chosen to be top/bottom symmetrical, and it is assumed that the field outside the box is zero, then the above equation can be written as

$$\frac{1}{\mu_{\text{garnet}}} \int_{\text{L}} \boldsymbol{B_M} \cdot d\boldsymbol{l} = \frac{B_M L}{\mu_{\text{garnet}}} = \mu_0 N_e I \tag{2.1.4}$$

where L is the length of the coil.

$$\mu_{\text{garnet}} = \frac{B_M L}{\mu_0 N_e I} \tag{2.1.5}$$

B_M can be determined by using both Faraday's Law and Lenz's Law,

$$V = -\frac{d\phi}{dt} \tag{2.1.6}$$

where ϕ is the magnetic flux in the material and V is the induced voltage in the measurement coil. In this setup, the relationship between ϕ and B_M is

$$\phi = N_m \int_A \boldsymbol{B_M} \cdot d\boldsymbol{A} = N_m B_M A \tag{2.1.7}$$

where $\boldsymbol{B_M}$ is parallel to the measurement coil, which has N_m turns and cross-sectional area $\boldsymbol{A}$. Because A is a constant, substituting equation 2.1.7 into 2.1.6, gives the following,

$$V = -N_m A \frac{dB_M}{dt} \tag{2.1.8}$$

and B_M is found by integration of the measured voltage using equation 2.1.9.

$$B_M = -\frac{1}{N_m A} \int_0^t V \, dt \tag{2.1.9}$$

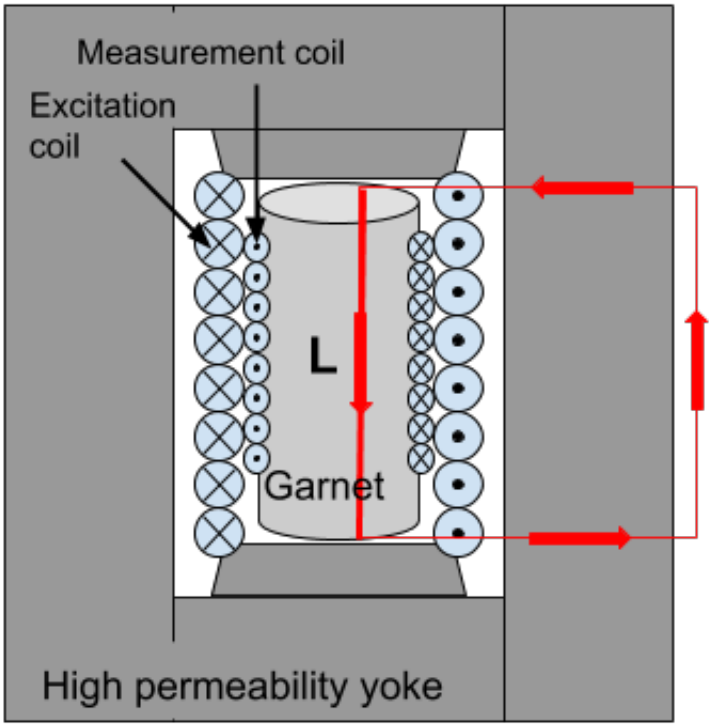

Figure 2.2: A cross-sectional view of the witness sample test apparatus flux return box, solenoid, and witness sample. The red rectangle is the closed loop integration path for applying Ampere's Law. The tightly fitted pole pieces at the end of the solenoid ensures that no field leaks into air gaps between the solenoid and the yoke.

Finally, equation 2.1.9 can be substituted into equation 2.1.5 to obtain an expression for μ_{garnet} in terms of the voltage measured in the measurement coil.

$$\mu_{\text{garnet}} = -\frac{L}{\mu_0 N_e N_m I A} \int_0^t V \, dt \tag{2.1.10}$$

With some modification, which will be discuss in section 2.5, equation 2.1.10 is used to determine the relative permeability of the AL-800 garnet witness samples.

2.2 Witness Sample Test Method Development

The development of the witness sample test method was an iterative process. At the onset, the immediate goal was to determine if a desktop setup could be designed that would adequately measure the *BH* curve of ferrite or garnet material. For budgetary reasons, it was necessary to use materials and equipment on hand or low cost retail products. In order to implement the witness sample test apparatus design, which will be discussed in section 2.3, a circuit needed to be developed that would excite the magnetic field in the samples and measure the corresponding magnetic flux.

The first measurement attempt was made on a ring of G-510, an aluminum doped, yttrium-iron garnet, manufactured by Trans-Tech Inc. The G-510 ring was wrapped with two layers of wire to make a measurement coil (96 turns) and an excitation coil (97 turns). Figure 2.3 shows the initial test circuit design. The circuit was designed as a proof of principle, and many features were ultimately changed. The drive signal was a 1 kHz sine wave and the amplifier was an Audiophile 5 watt audio amplifier. The 1 kHz drive signal was an arbitrary choice that was later refined to 180 Hz in order to match previous measurements. Voltage was measured across an 8 ohm shunt resistor to ground. An integrator circuit was considered on the measurement side, but was discarded in favor of post-measurement numerical integration. The numerical integration gave the same results as the integration circuit but had the advantage of not imposing limits on the measurement frequency.

Measurements with the initial circuit yielded an unexpected result. They showed that small DC biasing in the circuit could have dramatic effects on the calculations and would need to be accounted for in the analysis. Potential sources of DC bias in the circuit were determined to be

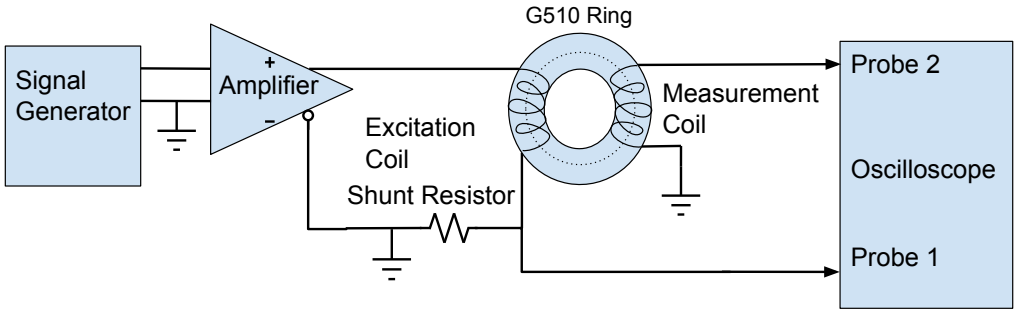

Figure 2.3: The initial garnet test circuit design.

a DC offset in the excitation signal out of the amplifier, remnant magnetization in the material from previous measurements, and a DC offset in the oscilloscope. Figure 2.4 shows the difference between the DC bias corrected and uncorrected data in the *BH* curve calculation for a multi-cycle measurement of the G510 ring in the test circuit.

The next step in the process was to measure a sample of AL-800 garnet in the test circuit. Measurements of the static permeability of AL-800 sample rings had been previously done by R. Madrak, G. Romanov, and I. Terechkine (FNAL) [11]. One of these AL-800 sample rings was prepared with coil windings like the G510 ring above, with 250 on excitation coil and 259 turns on the measurement coil. The test circuit was modified with a higher power amplifier, and a lower shunt resistance (4 ohm). These changes allowed a maximum bias field of 91 Oe. Figure 2.5 shows the measured *BH* curve of the AL-800 sample ring.

The increased bias field strength was still far below the desired strength of 2300 Oe for the witness sample test, however it was high enough that it allowed for a rough comparison of the test circuit results with the above mentioned static permeability measurements. Figure 2.6 shows the permeability of the AL-800 sample ring along with the static permeability results from R. Madrak *et al.* In the region of interest of $B > 800$ G, the AL-800 ring results on the test circuit showed agreement with the static permeability measurements. At this point, it was clear the test circuit would work well for measurement of the AL-800 witness samples with some adjustments to allow for more power. The final version of the measurement circuit will be detailed in Section 2.4.

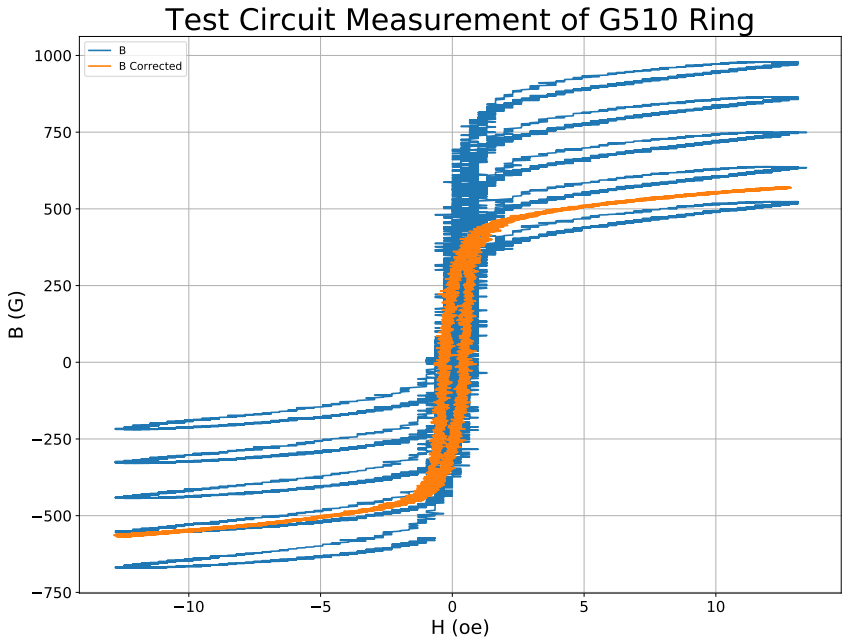

Figure 2.4: BH curve of the G510 ring in the test circuit with DC bias corrected and uncorrected.

2.3 The Witness Pieces and Measurement Setup

Each garnet ring is made up of eight sectors glued together with a 3 mm thick alumina ring base as shown in Figure 2.7. The witness samples measure 17.8 mm in diameter and 16 mm long. Figure 2.10 shows an example of a witness sample. The test apparatus was designed to provide a uniform magnetic field within the sample throughout the tested bias current range of 0 to 19.1 A. [12] Figures 2.8 and 2.9 show the cross-sectional design of the witness sample test apparatus, and the simulated B field lines during testing.

The witness sample test apparatus consists of the witness sample to be tested, a measurement coil that fits closely around the sample, an excitation coil that surrounds the measurement coil, and a flux return box that encloses everything. The flux return box is made of MN-60 ferrite, which has a high relative permeability of 6000, and ensures that the H-field is concentrated and uniform in the sample. Figure 2.11 shows the garnet witness sample test stand at different stages of assembly. The excitation and measurement coils were wound to fit inside the measurement

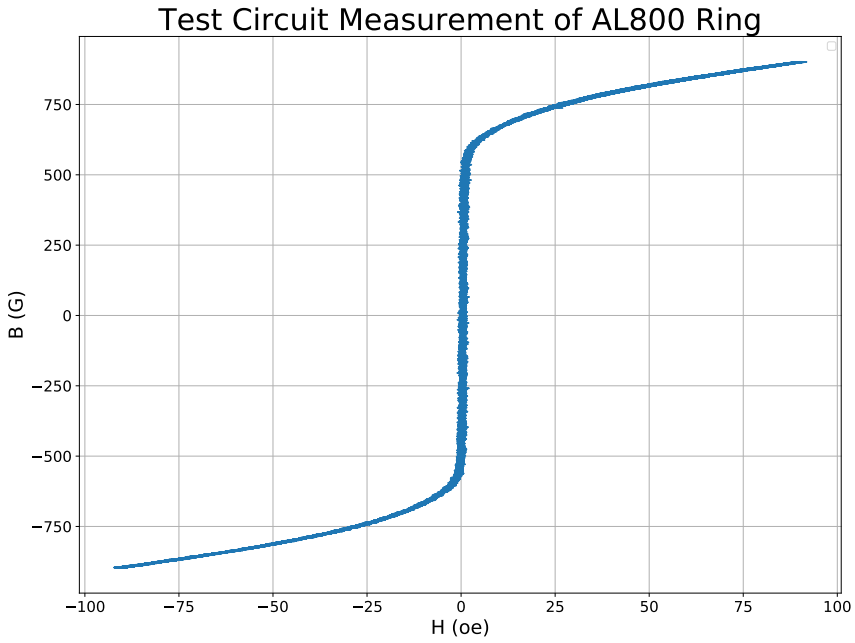

Figure 2.5: Measurement of an AL-800 garnet sample ring over multiple cycles showing the narrow *BH* curve.

box with the excitation coil surrounding the measurement coil. The measurement coil must fit as closely around the sample as possible. The excitation coil was wound with 183 turns of #14 (⌀0.62 mm) insulated copper wire, and the measurement coil with 80 turns of #34 (⌀0.16 mm) insulated copper wire. The measurement coil was wound to match closely the diameter of the samples while still allowing the samples to be easily placed inside. Both windings were done on a device with a turn counter to ensure an accurate turn count, as shown in Figure 2.12(b). The winding device was designed and built by T. Johnson (FNAL).

The coils were wound around spools, shown in Figure 2.12(a), that were printed with an Ultimaker 2 Extended+ 3D printer. The printed spools measured 20.3 mm in diameter for the excitation coil and 17.8 mm in diameter for the measurement coil. The excitation coil was wound around the larger spool and a layer of Kapton® tape (0.12 mm thick), which served as a base to which the first layer of wire would adhere. After each layer of wire, quick cure epoxy was added to bind the wires together. Prior to the winding, the surface of the spool and end washers were coated in petroleum

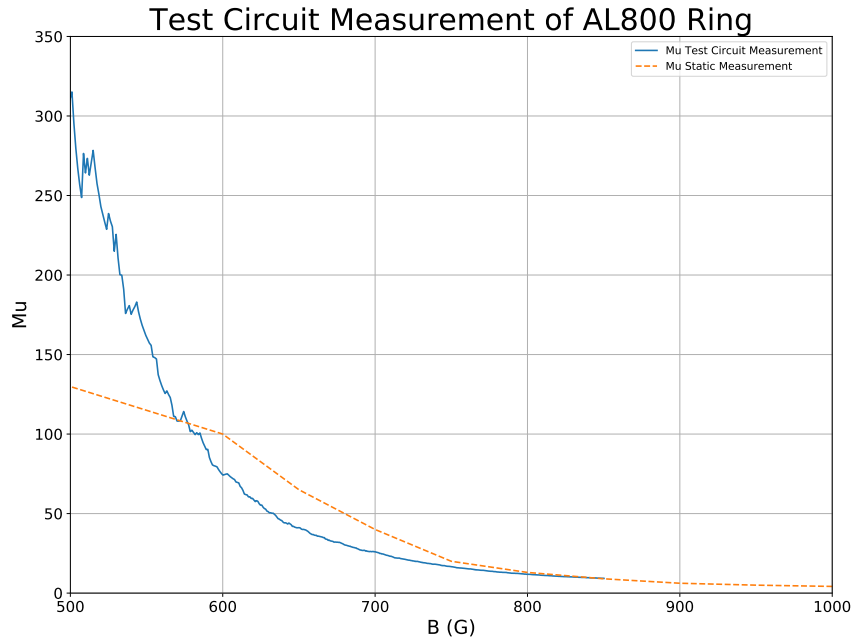

Figure 2.6: Measurement of an AL-800 garnet ring sample with previous results from static permeability measurements. The region of interest is above 800 G.

jelly to prevent the epoxy from adhering to the spool pieces. When the winding was completed and the epoxy was cured, the Kapton® tape was removed from the inner radius.

The measurement coil was prepared using the same method as the excitation coil, but with an additional layer of Kapton® tape. This extra layer of tape was not removed and served as a support structure for the much thinner wire. Although the dimensions were chosen to fit the witness samples, it was found that when the measurement coil was wound using only one layer of tape, the finished coil was too small to easily fit around the witness samples and would therefore be damaged after repeated measurements. Winding the coil around the additional layer of tape allowed samples to be easily placed and removed from the measurement coil but resulted in a small air gap between the samples and the measurement coil. This small air gap was accounted for in the analysis calculations.

Several steps were taken to ensure repeatability of the measurements. First, non-magnetic supports were placed under the excitation coil in the test apparatus to ensure that the position of

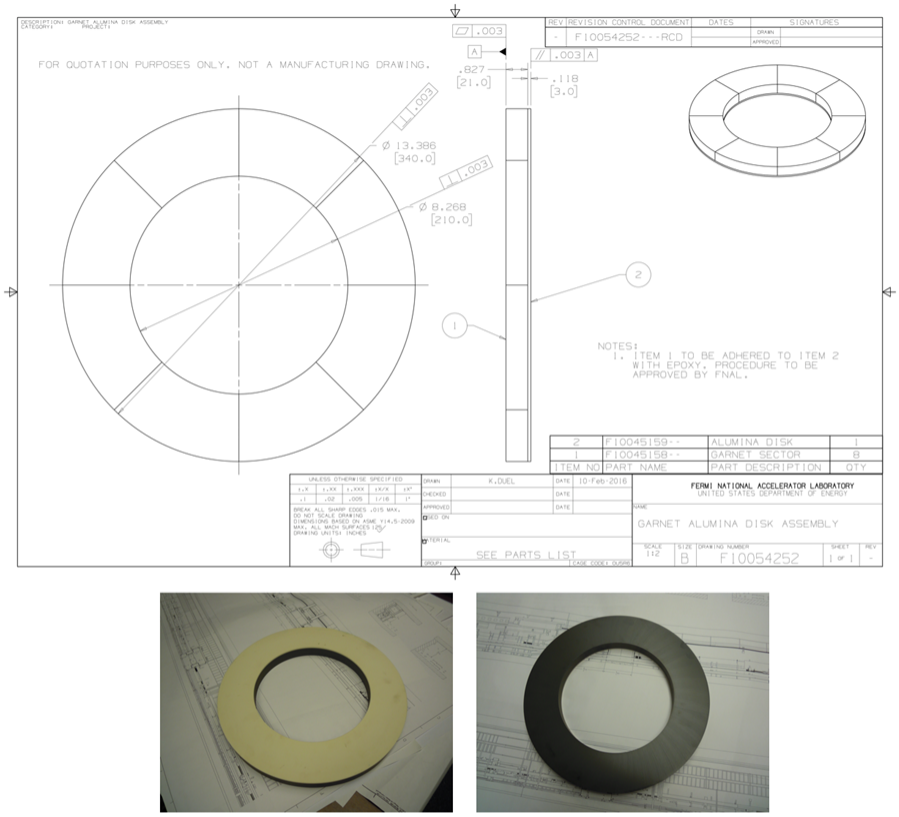

Figure 2.7: The garnet rings are made of 8 sectors of garnet epoxied together upon an alumina base.

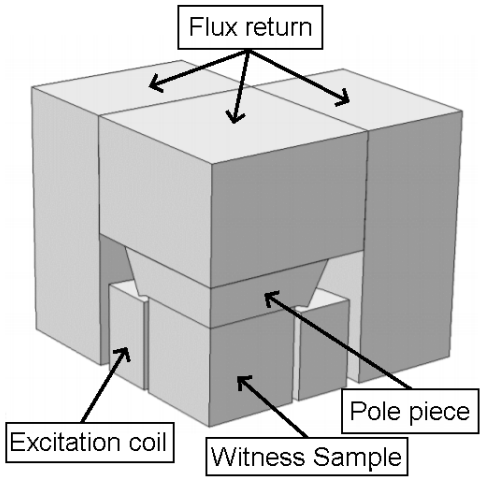

Figure 2.8: A 1/8th cross-sectional diagram of the witness sample test apparatus design. Image used with permission from I. Terechkine.

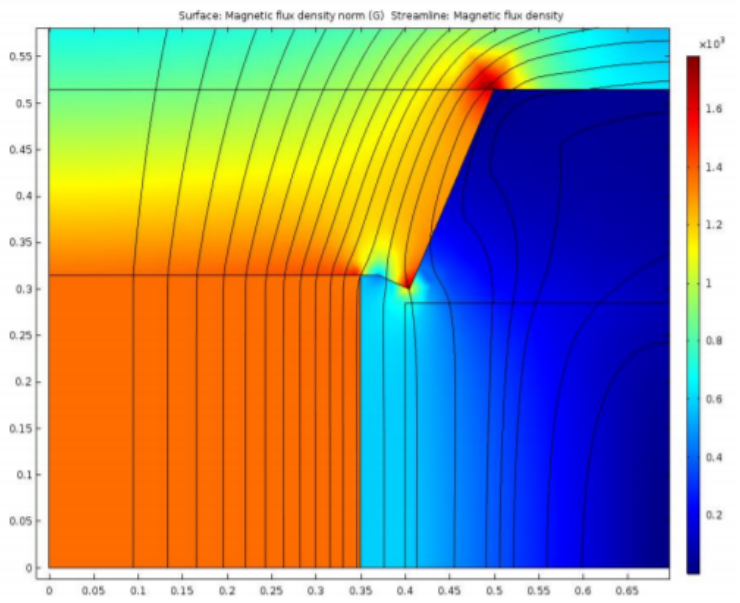

Figure 2.9: The witness sample apparatus was designed to have a uniform field in the samples. Image used with permission from I. Terechkine.

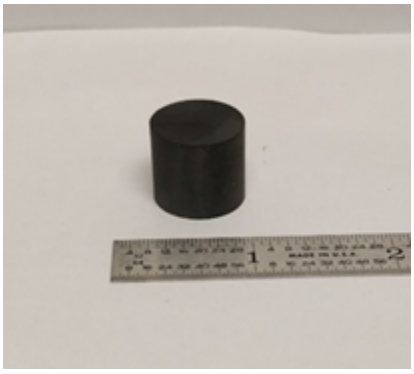

Figure 2.10: An example of an AL-800 witness sample. The sample is a cylinder 16 mm long and 17.8 mm in diameter.

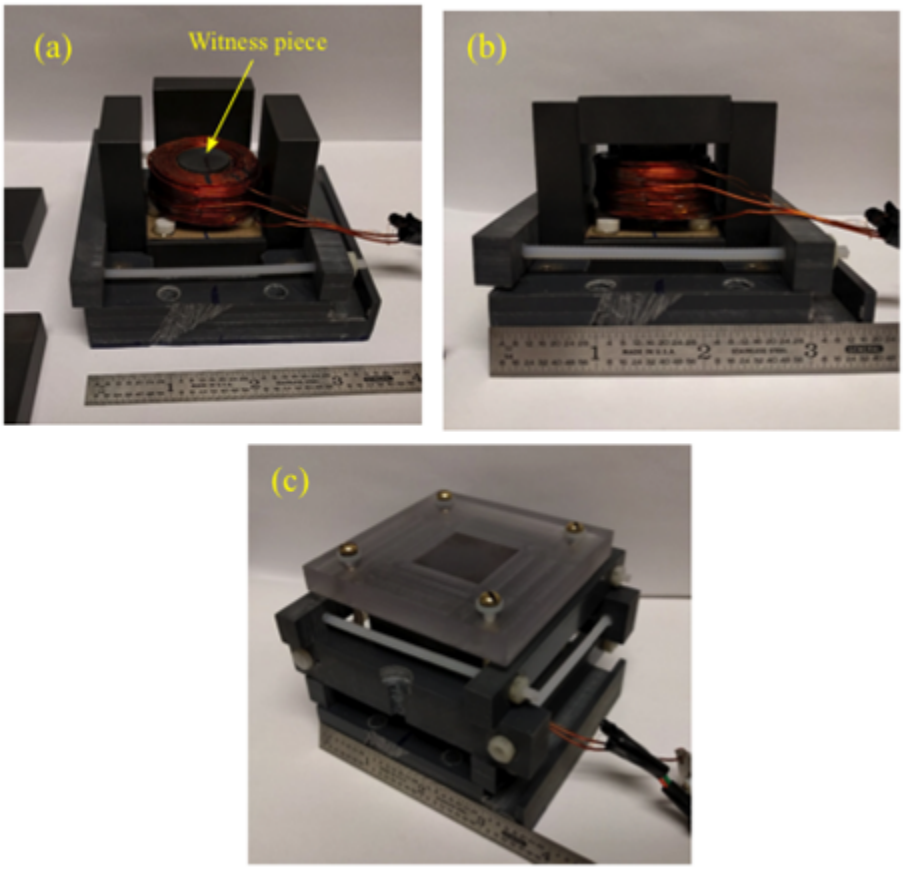

Figure 2.11: The garnet witness sample test stand at different stages of assembly. (a) The sample sitting in the partially assembled ferrite box. (b) The top cover is on. (c) The test stand fully assembled.

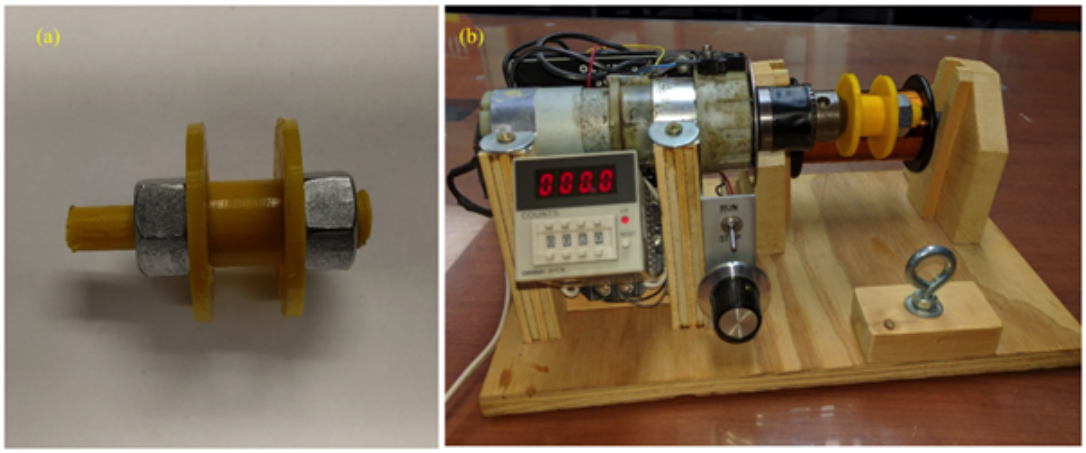

Figure 2.12: (a) is an example of a 3D printed spool piece and (b) is the winding device with its integrated counter.

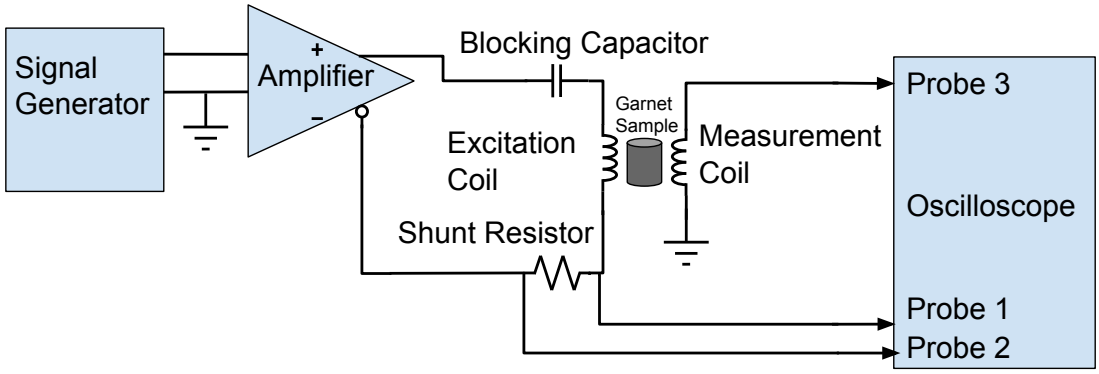

Figure 2.13: The witness sample measurement circuit showing probe connections.

the excitation coil relative to the samples was repeatably centered and level for each measurement. Second, the coils, flux pieces, and measurement samples were all marked to ensure repeatability during assembly and alignment of the apparatus. The apparatus was held together with clamps made from PVC and acrylic to minimize movement and to improve contact between the pieces of the ferrite flux return. The clamps had to be tightened carefully for each measurement. If the clamps were too loose, vibration during the measurement pulse would affect the measurement and possibly damage the sample. Overtightening the vertical clamp would result in damage to the samples from the downward compression.

2.4 Circuit and Measurement Technique

The sample measurement circuit is shown in Figure 2.13. The bias AC field was generated by an Agilent 33250A signal generator and amplified by the Behringer iNuke 6000 amplifier, which can generate currents up to approximately 20 A in the excitation coil. This current was measured using a precisely known shunt resistance (R = 3.92 Ω). A 1000 μF blocking capacitor prevented the unwanted DC offset of the current from biasing the magnetic circuit. It was found that this DC bias, if not removed, would result in substantial distortion of the measurement results.

The excitation current and the voltage generated in the measurement coil were recorded using a Tektronix TDS5054B-NV digital oscilloscope. Before each measurement, the sample was demagnetized using a decaying 180 Hz sine wave with the initial amplitude of the current 25% greater

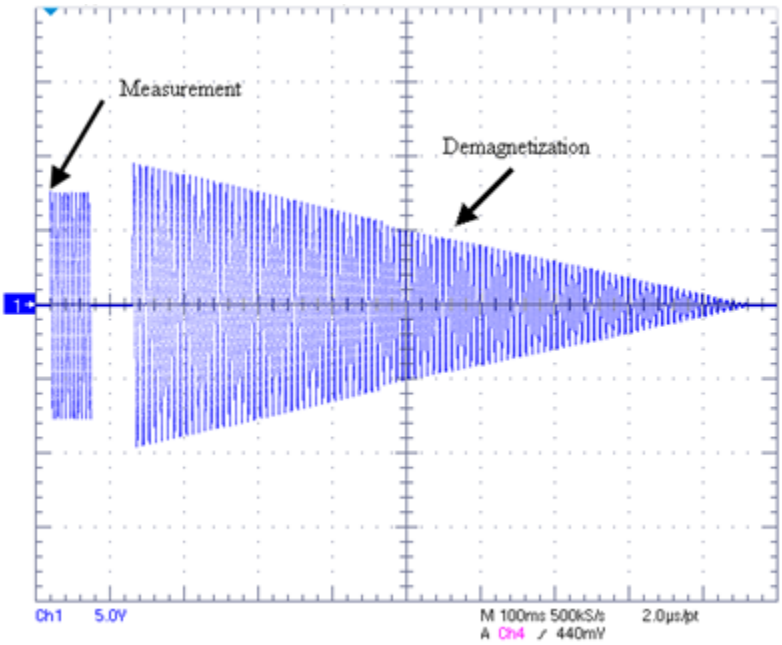

Figure 2.14: A typical measurement and demagnetization cycle. The demagnetization current is a decaying sine wave that starts with a current that is 25% higher than the measurement current.

than the maximum current used in the previous measurement cycle. Figure 2.14 shows a typical measurement and demagnetization cycle. After each cycle, the apparatus was taken apart and the sample inverted for the next measurement to counter any remnant magnetization and to avoid introducing other systematic errors due to the orientation of the material. The excitation current during the measurements was a 180 Hz sine wave with a peak current of 19.1 Amps. The measurements were taken during the first quarter of the sine wave from zero amps to peak current. During the measurements, the voltage to ground was measured at either side of the shunt resistor (probes 1 and 2 in Figure 2.13) and across the measurement coil (probe 3). The difference between the voltages on probes 1 and 2 was used to calculate the current and magnetic field strength H, using equation 2.1.3. It was necessary to do a differential measurement because neither side of the amplifier output was grounded. The measured voltage across the measurement coil allowed the calculation of the magnetic flux through the sample by numerical integration using equation 2.1.10 with a correction for the air gap which will be discussed in section 2.5.

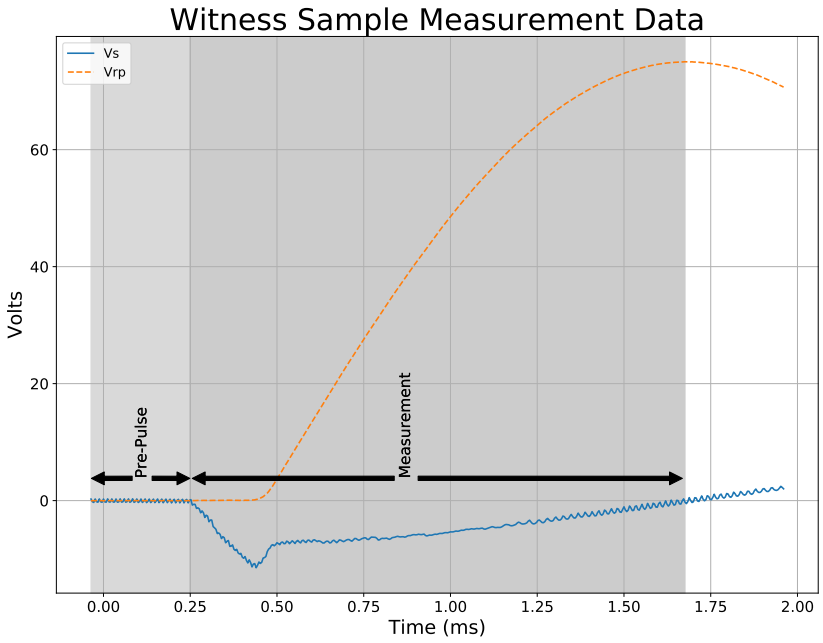

Figure 2.15: A typical measurement result showing the two data sets. V_s is the voltage across the measurement coil. V_{rp} is the voltage difference across the shunt resistor. The DC offset correction is calculated from the pre-pulse flat region at the beginning of the each data set.

2.5 Witness Sample Analysis

Each measurement resulted in two sets of data shown in Figure 2.15. The first is the difference between the voltage on the probes on either side of the shunt resistor, V_{rp}, and the second is the voltage across the measurement coil, V_s. The analysis calculations of the data was done with a Python 2.7 script written for that purpose. The analysis code is included in Appendix A. Both data sets have a small DC offset that must be subtracted. The DC correction is made by taking the average of the pre-pulse offset and subtracting it from the entire data set.

The magnetic field strength is calculated from Equation 2.1.3 above, which becomes

$$H = \frac{N_e V_{rp}}{LR} \tag{2.5.1}$$

where $N_e/L = 183/(18.2 \pm 0.8\ \text{mm})$ is the turn density of the excitation coil, and $R = 3.92\ \Omega$ is the shunt resistance.

B is calculated with equation 2.1.9 above,

$$V_s = -N_m A \frac{dB}{dt} \tag{2.5.2}$$

where $N_m = 80$ is the number of turns in the measurement coil and $A = 264\ \text{mm}^2$ is the cross-sectional area. The diameter of the measurement coil is larger than the diameter of the witness samples which creates a small air gap between them. This air gap is accounted for by separating the terms for the air gap and the garnet.

$$V_s = -N_m \left(A_{\text{air}} \frac{dB_{\text{air}}}{dt} + A_{\text{garnet}} \frac{dB_{\text{garnet}}}{dt} \right) \tag{2.5.3}$$

$$\int_0^t V_s\, dt = -N_m \left(A_{\text{air}} B_{\text{air}} + A_{\text{garnet}} B_{\text{garnet}} \right) \tag{2.5.4}$$

$$B_{\text{garnet}} = -\frac{1}{N_m A_{\text{garnet}}} \int_0^t V_s\, dt - \frac{A_{\text{air}} B_{\text{air}}}{A_{\text{garnet}}} \tag{2.5.5}$$

In the air gap,

$$B_{\text{air}} = \mu_0 H \tag{2.5.6}$$

The equation then becomes,

$$B_{\text{garnet}} = -\frac{1}{N_m A_{\text{garnet}}} \int_0^t V_s\, dt - \frac{A_{\text{air}} \mu_0 H}{A_{\text{garnet}}} \tag{2.5.7}$$

Integration of V_s is done numerically using a trapezoidal Riemann sum,

$$B_{\text{garnet}} = -\frac{1}{N_m A_{\text{garnet}}} \left[\sum_{i=0}^{n-1} \frac{V_{s,i} + V_{s,i+1}}{2} \Delta t \right] - \frac{A_{\text{air}} \mu_0 H}{A_{\text{garnet}}} \tag{2.5.8}$$

where the integration time has been divided into n equal intervals of $\Delta t = 4.00\ \mu\text{s}$, and $V_{s,i} = V_s(i\Delta t)$.

With the above expression for B_{garnet} and having previously calculated H from equation 2.5.1,

the relative permeability of the garnet is then found using equation 2.1.2.

$$\mu_{\text{garnet}} = \frac{B_{\text{garnet}}}{\mu_0 H} \tag{2.5.9}$$

$$\mu_{\text{garnet}} = -\frac{1}{N_m A_{\text{garnet}} \mu_0 H} \left[\sum_{i=0}^{n-1} \frac{V_{s,i} + V_{s,i+1}}{2} \Delta t \right] - \frac{A_{\text{air}}}{A_{\text{garnet}}} \tag{2.5.10}$$

$$\boxed{\mu_{\text{garnet}} = -\frac{LR}{N_e N_m A_{\text{garnet}} \mu_0 V_{rp}} \left[\sum_{i=0}^{n-1} \frac{V_{s,i} + V_{s,i+1}}{2} \Delta t \right] - \frac{A_{\text{air}}}{A_{\text{garnet}}}} \tag{2.5.11}$$

2.6 Witness Sample Results

As stated previously, the goal for testing the garnet witness samples was to determine whether the magnetic permeability of the samples is near the specification value as given by the manufacturer, Table 2.1, and whether all the samples have the same permeability, within 5% of each other. In total, 83 witness samples from five different lots were tested. Each lot represents a manufacturer's production batch that has slightly different properties as reported by the vendor in Table 2.1 below. The vendor data and the witness sample measurement results are presented in cgs units of gauss and oersted. The vendor data was obtained from measurements made with a Powdertech International Powderfluxmeter-QC device, which uses a static magnetic field and a sample of the powdered garnet before it has been sintered.

Lot #	Sample Count	Segment #	ϵ'	tan δ_ϵ	$4\pi M_s$ (G)	Line Width (Oe)
62800	24	Shims	13.83	0.0001	767	26.0
66747	17	1 to 17	13.76	0.0001	765	28.6
66962	26	18 to 43	13.78	0.0001	780	29.0
67232	13	44 to 67	13.93	0.0001	776	21.3
67366	3	68 to 72	13.81	0.0001	778	19.98

Table 2.1: Witness sample data as provided by the vendor.

The measured B, H, and permeability for a single sample are shown in Figures 2.16 and 2.17. Figure 2.17 shows the statistical and systematic measurement uncertainty, which is large and variable at $B < 800$ G, and very small for $B > 800$ G. The uncertainty is dominated by the statistical effects. The results for Sample 2 are typical for all of the witness samples. One can see in these

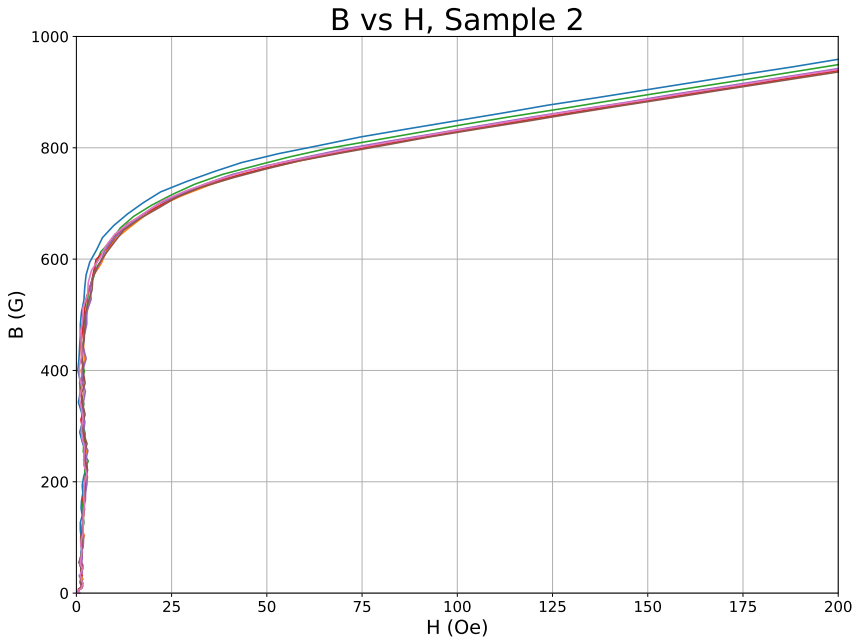

Figure 2.16: B vs H for a single witness sample.

plots that the test setup is not sensitive in the region $B < 800$ G due to noise in the system and the sharp rise in $B(H)$ at low H. However, at $B > 800$ G, the data converges and some conclusions can be made. Figures 2.18, 2.19, 2.20, 2.21, 2.22, and 2.23 show the permeability results for each witness sample lot and the aggregate of all samples in the region of interest, $B > 800$ G.

In order to compare the witness sample measured results with the vendor data, it is necessary to calculate the magnetic saturation, $4\pi M_s$, of each sample lot. The data can be fitted to the model with an offset $\Delta\mu$ that ensures the fit converges to $\mu = 1$.

$$\mu(B) = \frac{1}{1 - \frac{4\pi M_s}{B}} + \Delta\mu \tag{2.6.1}$$

Fitting the data to this model must be done post saturation, when the magnetization of the material is constant. This presented a challenge because the fit results were highly dependent on the minimum B value included in the fit. For example, if the fit was performed on the range 800 G $< B <$ 3000 G, the $4\pi M_s$ fit result was different than the fit result on the range 850 G $< B <$ 3000

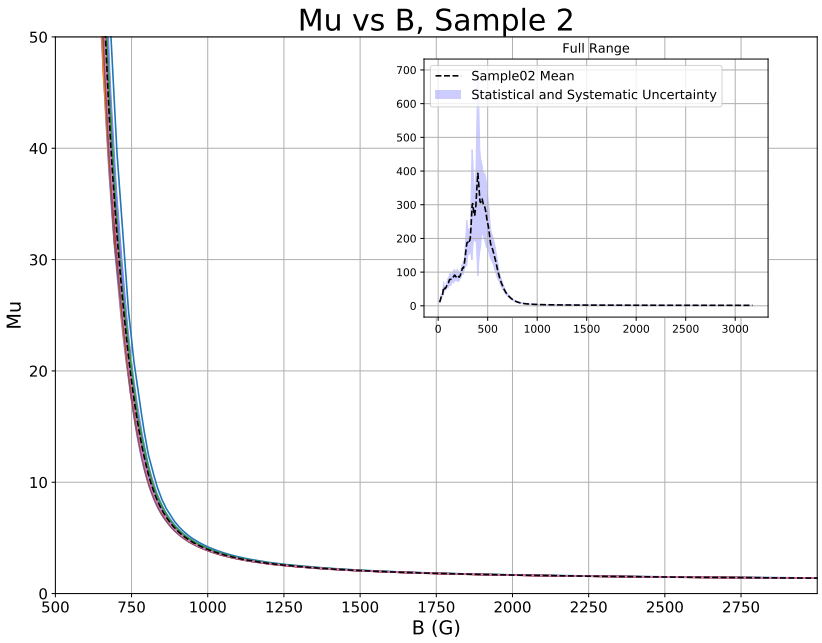

Figure 2.17: Relative permeability vs B field for a single witness sample.

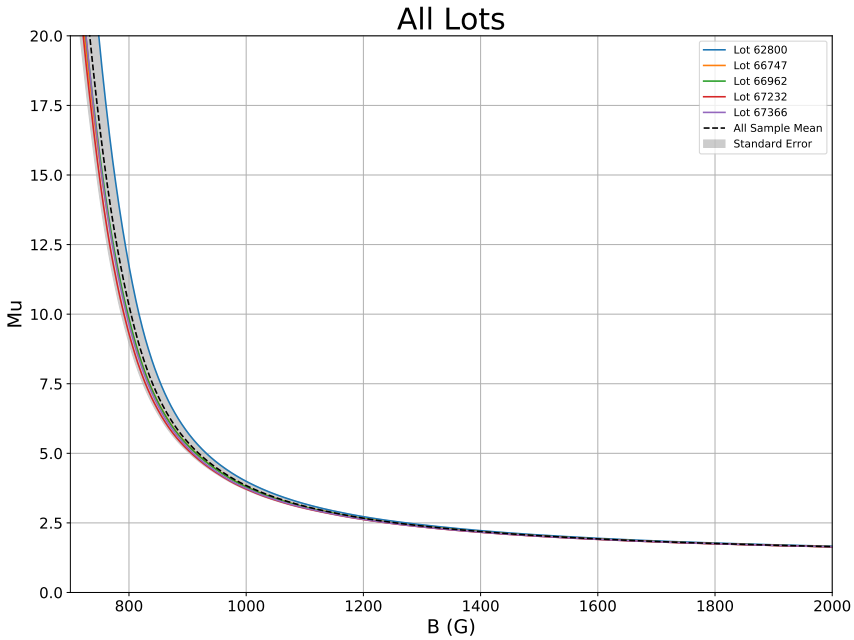

Figure 2.18: Permeability results for all witness sample lots.

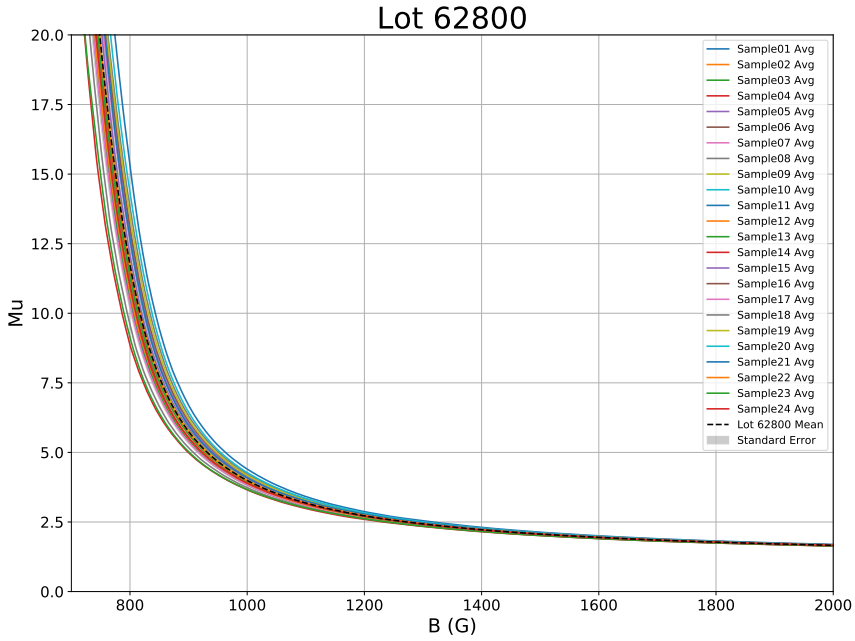

Figure 2.19: Permeability results for lot 62800.

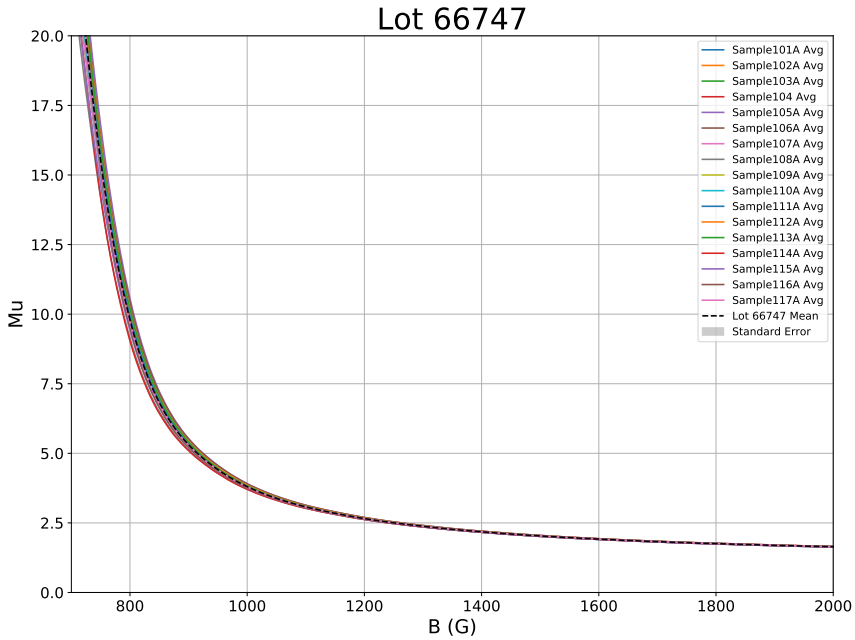

Figure 2.20: Permeability results for lot 66747.

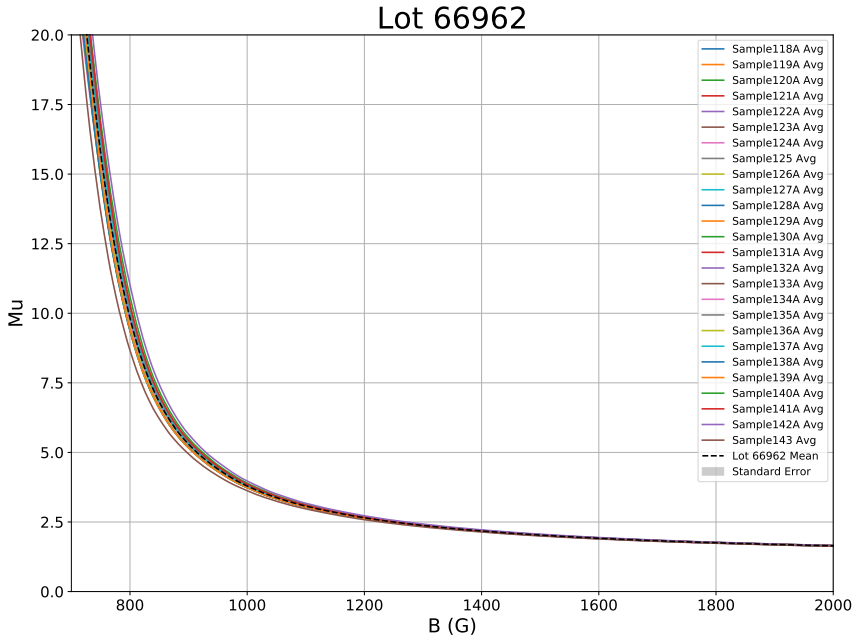

Figure 2.21: Permeability results for lot 66926.

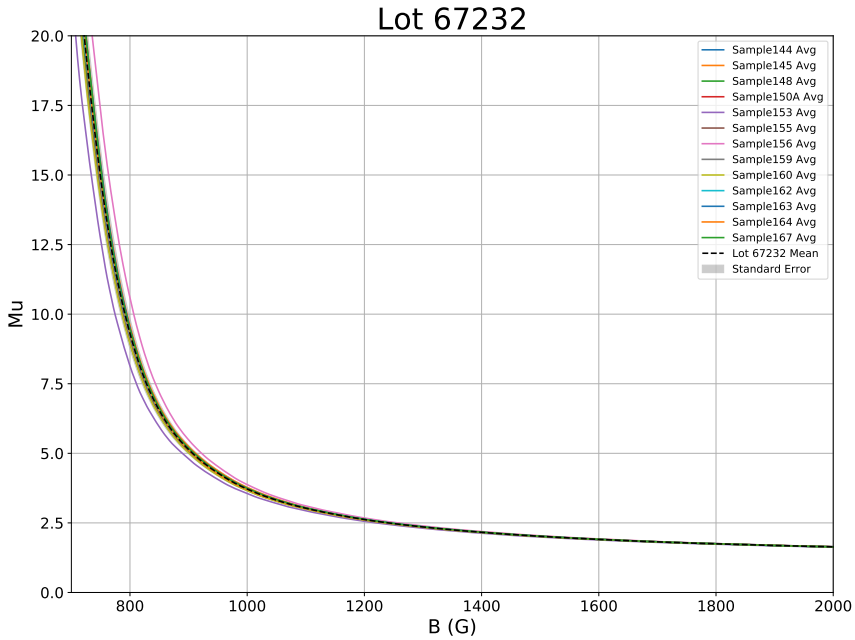

Figure 2.22: Permeability results for lot 67232.

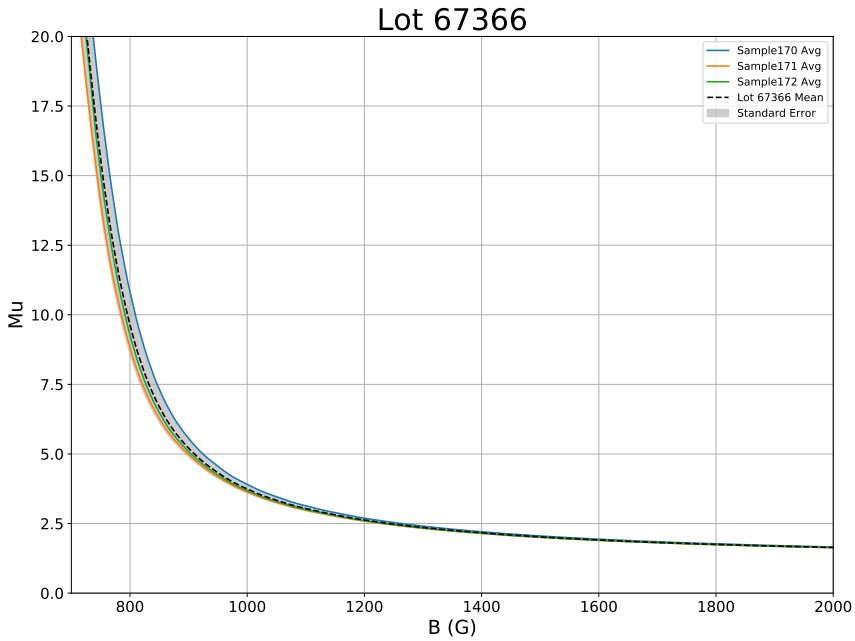

Figure 2.23: Permeability results for lot 67366.

G, or any other range of B as defined by the minimum B of the fitted data. An objective metric was needed to determine which portion of the data set should be fitted for the $4\pi M_s$ calculation.

One option for overcoming this problem was to fit the data for all possible ranges as a function of the minimum B and select the range to be fitted based on the results with the minimum fit error. This option was not satisfactory as it resulted in an unreasonable portion of the data excluded from the fit.

The measured data can also be fitted to the post saturation relation of $B(H)$. This linear fit also includes an offset $\Delta\mu$.

$$B(H) = (1 + \Delta\mu)H + 4\pi M_s \tag{2.6.2}$$

The linear fit of $B(H)$ is also dependent on the minimum B value included in the fit.

Ideally, the results of the two fits to the data should be the same, and so for each lot, the $4\pi M_s$ was determined by selecting the range of data where the two fit methods were in agreement. For each sample, this resulted in a single value for $4\pi M_s$ that satisfied both fits, with a reasonable error and offsets calculation. Figure 2.24 shows the calculated $4\pi M_s$ vs the minimum B in the fitted

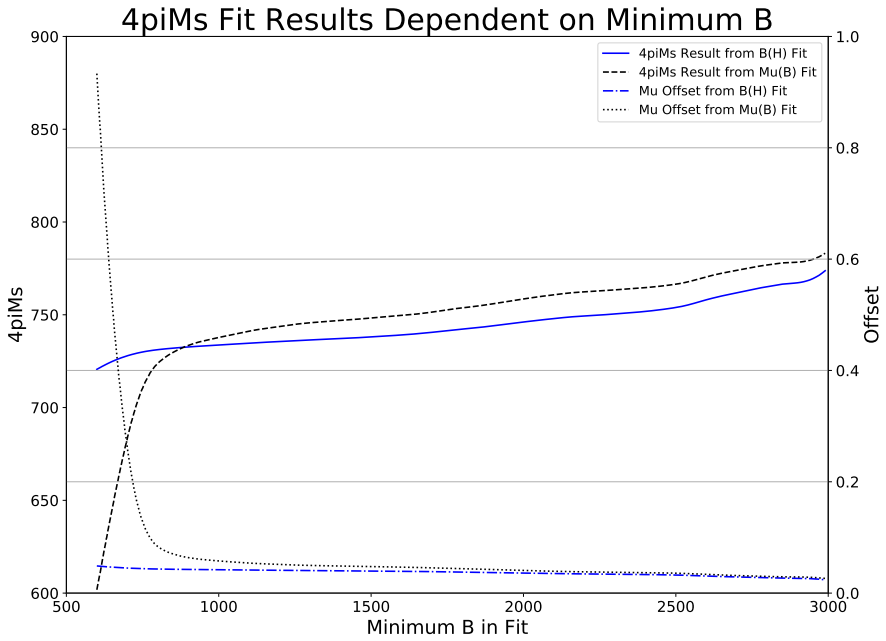

Figure 2.24: The calculated $4\pi M_s$ and $\Delta\mu$ offset from two fits of the data as a function of the minimum of the fitted data range.

data for both fits on the whole sample set. Table 2.2 shows the measurement results using this method alongside the material data supplied by the vendor. Table 2.3 shows the various measured quantities and their corresponding uncertainties that were a included in the data analysis.

Lot #	**$4\pi M_s$ Vendor (G)**	**$4\pi M_s$ Calculated (G)**	**$\Delta\mu$ Offset from $\mu(B)$ Fit**
All	772*	731.9 ± 3.9	0.062 ± 0.001
62800	767	743.6 ± 4.2	0.059 ± 0.002
66747	765	729.6 ± 3.9	0.061 ± 0.002
66962	780	728.3 ± 3.7	0.063 ± 0.002
67232	776	721.2 ± 3.6	0.067 ± 0.002
67366	778	720.6 ± 3.5	0.070 ± 0.005

Table 2.2: $4\pi M_s$ values as calculated from the measured data and provided by the vendor. Uncertainties are statistical and systematic combined. *Weighted average of the lots.

The $4\pi M_s$ values calculated from the measurement data for the sample lots are $3.1 - 7.4\%$ less than the vendor supplied data as can be seen in Figure 2.25. The vendor measures the $4\pi M_s$ of the powdered garnet material before sintering with a PowderTech PowderFluxmeter-QC. The meter

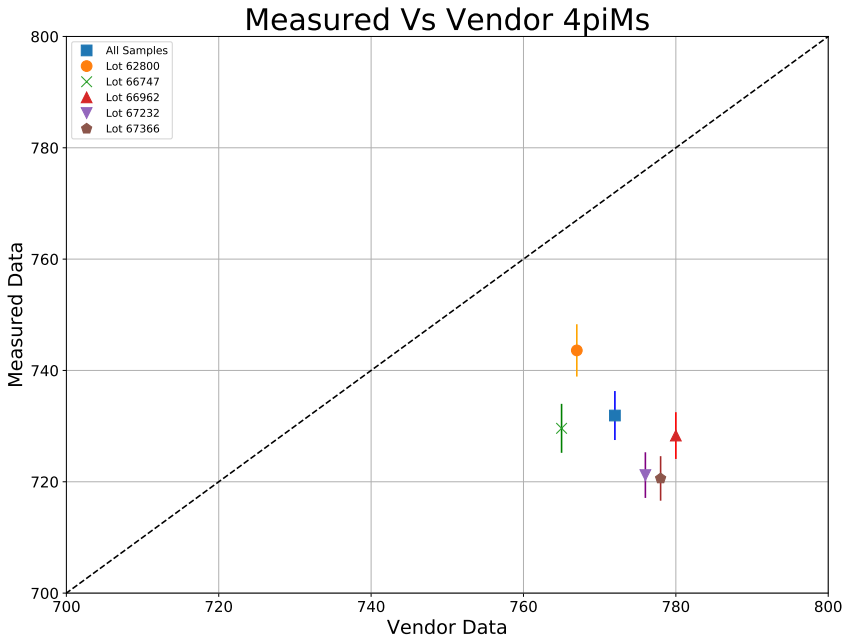

Figure 2.25: The measured $4\pi M_s$ compared to the vendor supplied $4\pi M_s$ values.

applies a magnetic field to the sample powder using strong permanent magnets and displays the magnetic saturation when the sample vial is pulled from the test chamber. As indicated in equation 2.5.11, the expected effect of sintering on the powder is an increase in permeability as the empty space between particles is removed and the density of the material increases. The opposite effect was seen in the measurement of the witness samples and the cause is not understood. However, the most important metric for evaluating the AL-800 witness samples was the spread in permeability between batches. The vendor data indicated a spread of 2.0% between batches and the measured results show a spread of 3.1%. While the measured spread is greater than expected, it is less than the 5% maximum threshold set by the cavity design team.

Measured Quantity		Units	Measured	Uncertainty
Excitation coil length	L	mm	18.2	± 0.8
Shunt resistor	R	ohm	3.92	± 0.01
Measurement coil diameter	d_c	mm	18.34	± 0.03
Sample diameter (variable)	d_s	mm	$17.64 - 17.81$	± 0.02
Voltage - shunt resistor	$V_{rp}(t)$	volt	75 (max)	$\pm 1.4 \times 10^{-6}$ *
Voltage - measurement coil	$V_s(t)$	volt	11 (max)	$\pm 1 \times 10^{-6}$ *

Table 2.3: Measured quantities and their absolute uncertainty. *Oscilloscope precision.

Chapter 3

Garnet Rings

The AL-800 garnet rings, shown previously in Figure 2.7, and below in Figure 3.1, are made of eight sectors of garnet epoxied together and then epoxied onto an alumina substrate that assists with heat dissipation. The rings are made from sectors because the manufacturer does not have a large enough oven to make the rings from one continuous piece of garnet. Figure 3.2 shows the canon at NMG used to press the powdered garnet into blocks. The testing of the witness pieces assured that the garnet sectors were sufficiently similar in magnetic permeability to be assembled into rings. The resonant frequency (f) and quality factor (Q) of the fully assembled rings were measured in the garnet ring test stand.

3.1 Garnet Ring Test Stand

The garnet ring test stand consists of a cavity and a bias solenoid, a Sorensen DCS60-20E power supply, a FLUKE 26 III True RMS Multimeter, an Agilent Technologies E5061B network analyzer, and an ENI 601L 1.2 watt linear RF amplifier. The current output of the Sorensen DCS60-20E power supply is measured with the multimeter across a 0.01 Ω resistor. A photograph of the test stand is shown in Figure 3.3. The cavity can be thought of as a quarter wave resonator with a large gap capacitance. The unloaded cavity resonant frequency is ~ 138 MHz. The bias solenoid consists of 224 turns of 10-gauge square copper wire and a flux return made of 1010 low carbon steel. A drawing of the test cavity and its photographs are shown in Figure 3.5.

After measuring the resonant frequency and Q of the empty test cavity, the same measurements were repeated with the cavity loaded with each garnet ring as a function of solenoid bias. The

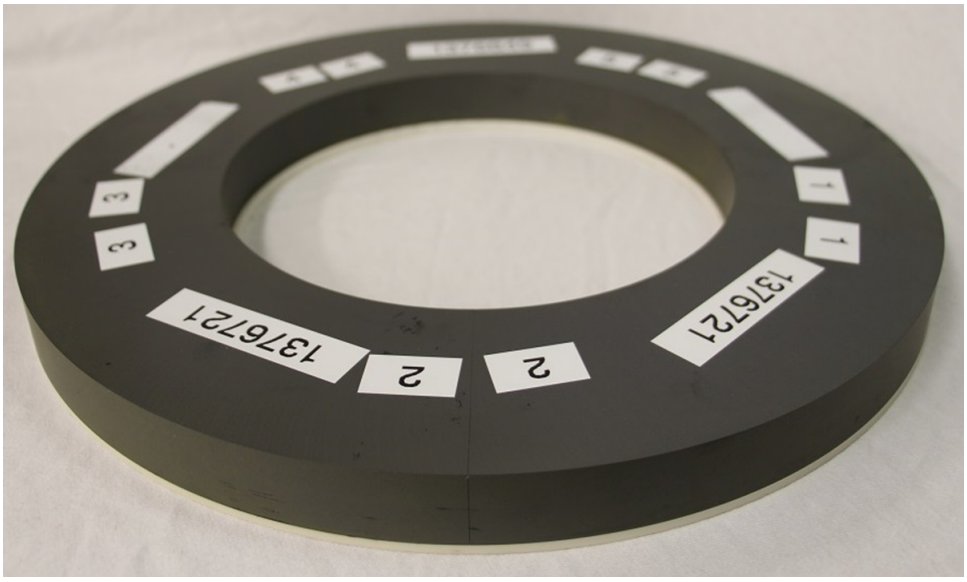

Figure 3.1: A garnet ring assembled from eight garnet sectors and the alumina substrate.

Figure 3.2: The canon at National Magnetics used to press the garnet powder into blocks.

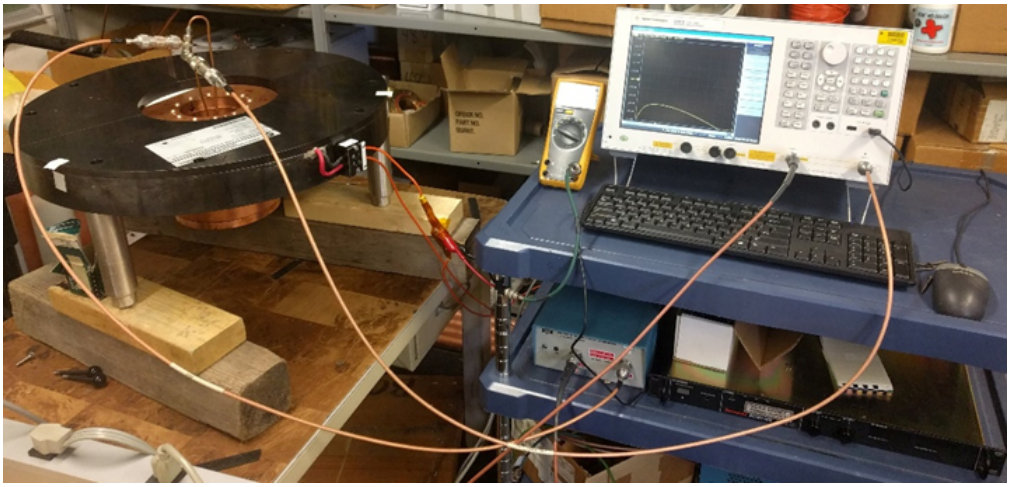

Figure 3.3: The garnet ring test stand. Here, the cavity is completely enclosed by a flux return.

resonant frequency range of the loaded cavity is 60 MHz to 121 MHz.

Initial measurements on the cavity indicated a lower than expected Q for both the loaded and unloaded conditions. The unloaded cavity simulations predicted an unloaded Q of 2200 and a loaded Q of 2400, but the initial measurement results showed an unloaded Q of 1294 ± 0.4. Likewise, the loaded cavity initial Q results were significantly lower than expected, with a range of 1300-1800 compared to the expected 2400.

It was determined that there were two possible issues with the cavity that could be causing a lower and inconsistent Q. First, the interior of the cavity had an anti-corrosion coating of KRYLON® Crystal Clear Acrylic Coating on the copper surface that was believed might be affecting the conductive skin depth. The coating was removed with Citristrip paint remover, but the measured Q did not significantly improve.

Second, it was hypothesized that the lid of the cavity might be making poor electrical contact with the cavity body. To improve the electrical contact, the 24 bolts that hold the cavity lid to the body were tightened to a torque of 40 ft-lbs ± 5% using an Express Assembly Electric Screwdriver ES-645L1 in a star pattern around the lid to avoid uneven contact. In addition, two 0.1710" x 0.0940" grooves were cut into the lid to allow for the placement of a gasket made from Spira Shield SS-08 - a spring temper, tin plated beryllium copper ribbon, as shown in Figure 3.6.

The addition of the Spira gasket and the consistent torque of the fastening bolts improved the

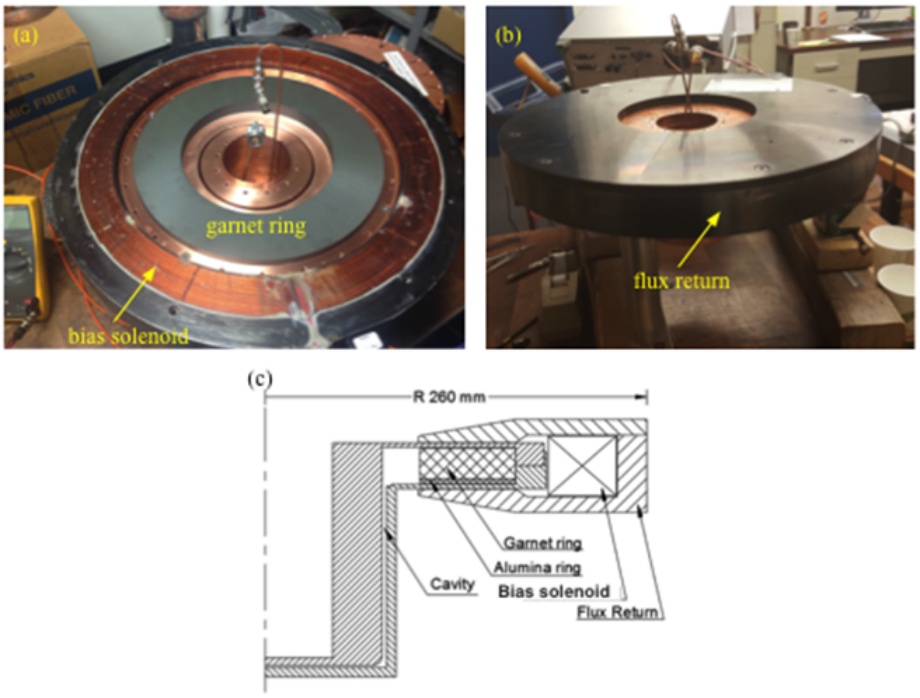

Figure 3.4: The garnet ring test stand and cross sectional schematic.

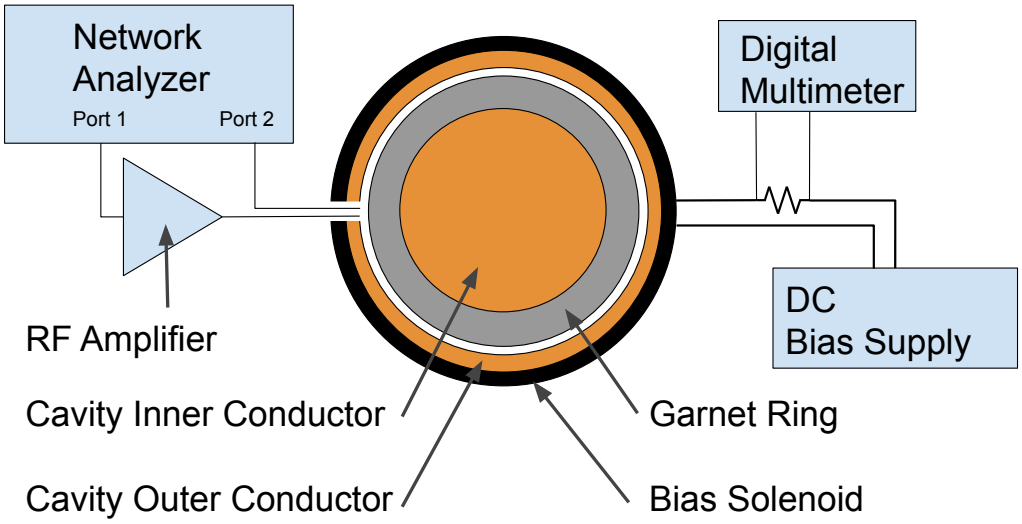

Figure 3.5: The garnet ring test stand circuit.

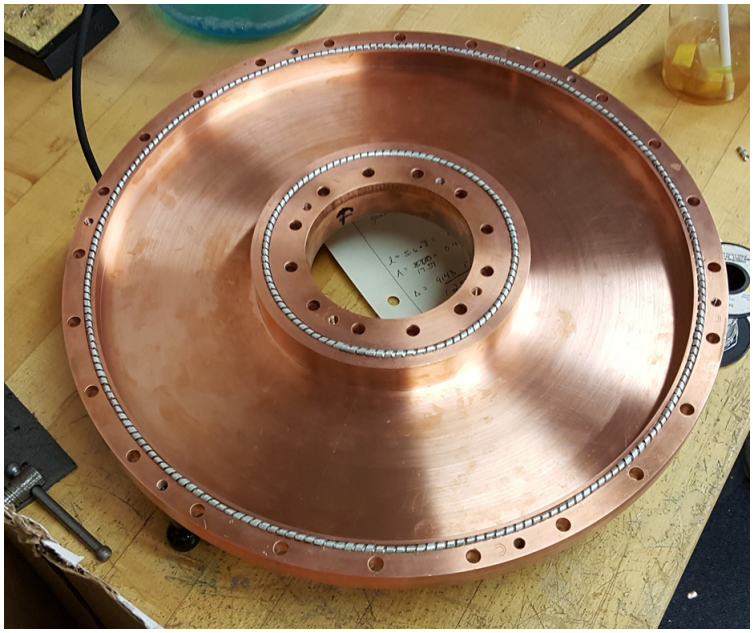

Figure 3.6: The garnet ring test cavity lid with Spira Shield SS-08 gaskets installed.

measurement results considerably. The Q of the unloaded cavity was 1860 ± 7, and the loaded cavity was 2113 ± 6. While the improved Q results were encouraging, it was curious that the loaded cavity had a higher Q than the unloaded cavity. The reason these results were surprising, despite the simulations predicting them, is that the typical result of adding a ferrite material to an RF cavity is a measured Q that is lower than that in the unloaded cavity. Later simulations by I. Terechkine showed that the cause of the surprising result was the geometry of the cavity and the permeability of the garnet [13]. When the bias field is below saturation of the garnet, the region of the cavity with the garnet has a greater permeability than the rest of the cavity. The presence of the garnet in the cavity changes the distribution of the field lines and as a result, the magnetic energy stored in the loaded cavity dissipates less power than in the unloaded cavity. Figure 3.7 shows the different field distributions in the loaded and unloaded cavity.

Figures 3.8 and 3.9 show the measurement results of the test cavity loaded with each of the garnet rings. As with the witness sample measurements, the most important consideration is the consistency of the garnet rings. While the average Q of the loaded cavity is still lower than the predicted value, the range of the measured maximum Q of the 5 garnet rings spans less than 3% of the mean average maximum Q. This result was considered acceptable and the garnet rings were

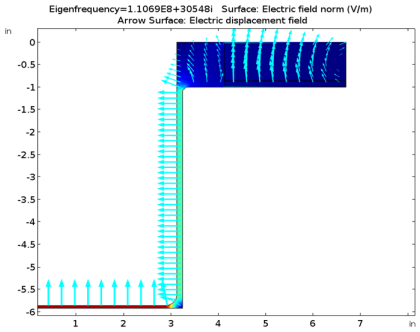

(a) Loaded cavity

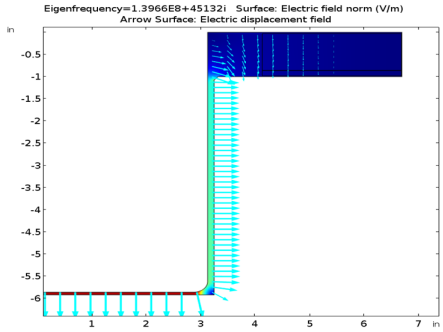

(b) Unloaded cavity

Figure 3.7: Simulations by I. Terechkine showing field line distribution in the loaded and unloaded cavity. Images used with permission.

certified for use in the cavity.

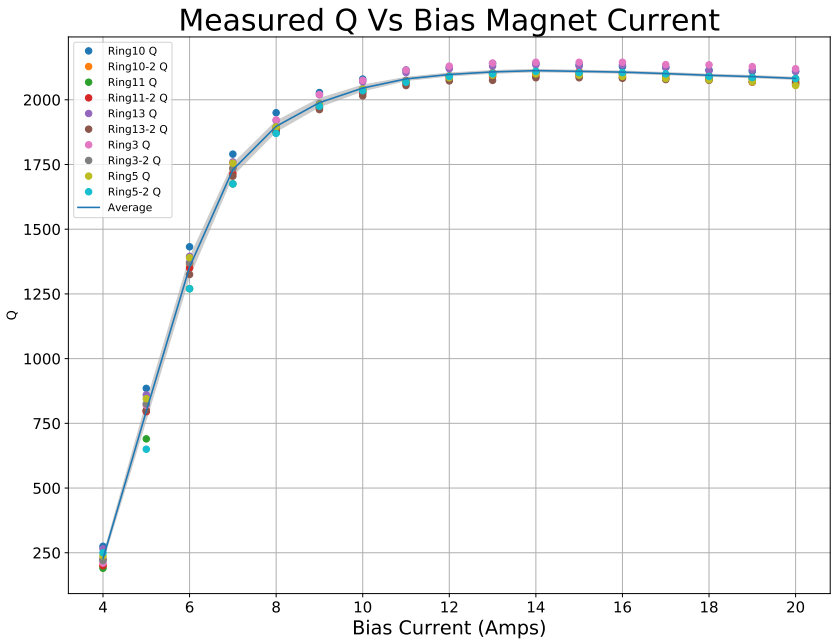

Figure 3.8: Measured Q of the cavity loaded with each of the five garnet rings as a function of bias current.

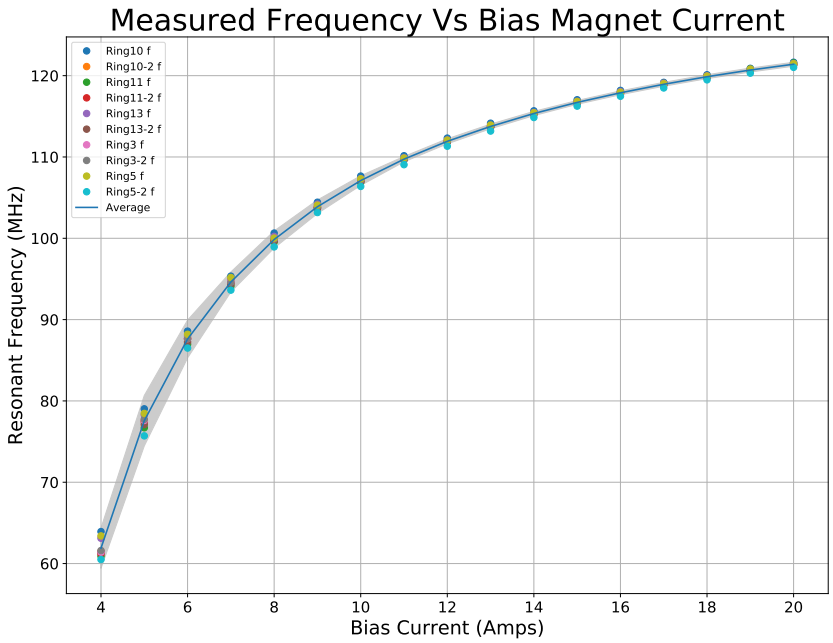

Figure 3.9: Measured resonant frequency of the cavity loaded with each of the five garnet rings as a function of bias current.

Chapter 4

Conclusion

Measurements of the properties of AL-800 garnet witness samples and fully assembled garnet rings show that the material is acceptable for use in the Booster 2nd harmonic cavity project. While there is confidence in the results, some questions remain and the witness sample test could be modified to possibly resolve those questions.

The witness sample measurements showed that the material manufacturing process yields a batch-to-batch variation of 3.3% for the measured $4\pi M_s$. The measured variation is less than the project's 5% threshold for acceptability, and it is close to the manufacturer's measured variation of 2.0%. The average measured magnetic saturation value was $2.9 - 7.3\%$ less than values provided by the manufacturer. The reason for the discrepancy between the measurement results and the manufacturers data is not known. The manufacturer's test is performed on the powdered sample, before the sintering process turns the material into a solid block. The solid samples are expected to have an increase in magnetic saturation compared to the powdered samples due to the elimination of empty space between sample particles. Since this is not what has been observed, it means that there is some unknown factor causing the discrepancy. Modification and improvement of the test setup and method, and additional testing of the witness samples might help resolve the discrepancy.

Although the witness sample test apparatus was designed to provide a uniform magnetic field in the sample, the excitation coil was not a perfect winding and perhaps contributed to a non-uniform field. A more precise winding of the coil would eliminate a possible variable.

Another possible improvement to the test apparatus would be a better mechanism for securing

the test box during each measurement. The implemented clamp design was effective at securing the test box, but the number of bolts required to secure the clamps made each measurement time consuming and subject to variation due to human error. A spring loaded top clamp was attempted, but ultimately rejected because the spring pressure was too little to be effective during the test, and was not easily manipulated by the operator. A better mechanism that could reliably and effectively lock the pieces of the apparatus into position, while still being easy to operate, would allow for more tests per sample and reduce variation between tests.

The witness sample test setup as described was not sensitive to the low field, pre-magnetic saturation region. The Behringer iNuke 6000 amplifier is an off the shelf audio amplifier that was chosen for its low cost and high current output. High frequency noise in the system contributed to the poor low field sensitivity. Filtering the high frequency noise could have improved the low field sensitivity, but at a cost of reducing the maximum current in the system. Alternatively, a different amplifier could be selected that had the desired output without the high frequency noise component.

The measurement and evaluation of the AL-800 garnet was a success. The test results showed that the garnet as manufactured by National Magnetics is acceptably uniform in magnetic properties and suitable for use in the 2nd harmonic cavity bias tuner. The experimental setup and test methods developed for this project can be implemented and built upon as part of ongoing work to evaluate other garnet materials.

Bibliography

[1] B. Worthel, J. Crawford, W. Pellico, J. Morgan, C. Gattuso, J. Reyna, B. Drendel, T. Sullivan, and C. Broy, "Booster Rookie Book." Available: https://beamdocs.fnal.gov/AD/DocDB/0010/001022/001/Booster %20V3_0.pdf, February 2004.

[2] F. Garcia, S. Chaurize, C. Drennan, K. Gollwitzer, V. Lebedev, W. Pellico, J. Reid, C.-Y. Tan, and R. Zwaska, "Fermilab - The Proton Improvement Plan (PIP)," in *HB2018* (G. Volker RW Schaa (GSI, Darmstadt, ed.), ICFA Advanced Beam Dynamics Workshop (61st), JACoW, July 2018.

[3] J. Dey, K. Duel, M. Kufer, J. Kuharik, R. Madrak, A. Makarov, R. Padilla-Dieppa, W. Pellico, J. Reid, G. Romanov, R. Scala, B. Schupbach, M. Slabaugh, D. Sun, C. Tan, and I. Terechkine, "A Perpendicular Biased 2nd Harmonic Cavity for the Fermilab Booster." Available: https://beamdocs.fnal.gov/AD-public/DocDB/ShowDocument?docid=6113, April 2018.

[4] R. Madrak, J. Dey, K. Duel, M. Kufer, J. Kuharik, A. Makarov, R. Padilla, W. Pellico, J. Reid, G. Romanov, M. Slabaugh, D. Sun, C. Y. Tan, and I. Terechkine, "The FNAL Booster 2nd Harmonic RF Cavity," in *HB2018* (G. Volker RW Schaa (GSI, Darmstadt, ed.), ICFA Advanced Beam Dynamics Workshop (61st), JACoW, July 2018.

[5] W. Weng and J. Kates, "Effects of the Second Harmonic Cavity on RF Capture and Transition Crossing," in *XVth International Conf on High Energy Accelerators*, (Hamburg, Germany), 1992.

[6] R. Poirier and T. Enegren, "Parallel Bias vs Perpendicular Bias of a Ferrite Tuned Cavity for the Triumf Kaon Factory Booster Ring," in *European Particle Accelerator Conference*, (Rome, Italy), 1988.

[7] Q. Mohaidat, M. Lataifeh, K. Hamasha, S. Mahmood, I. Bsoul, and M. Awawdeh, "The Structural and the Magnetic Properties of Aluminum Substituted Yttrium Iron Garnet." https://doi.org/10.1590/1980-5373-MR-2017-0808, May-Jun 2018.

[8] N. M. Group, "Garnet Materials." https://www.magneticsgroup.com/material/garnet/. Accessed: 2020-11-14.

[9] R. Madrak, "A new Slip Stacking RF System for a twofold Power upgrade of Fermilab's Accelerator Complex," *Nuclear Instrument and Methods in Physics Research*, vol. A758, no. 10, pp. 15–25, 2014.

[10] P. Coleman., F. Brandebeq, C. Friedrichs, Y. Goren, T. Gri, G. Hulsey, S. Kwiatkowski, A. Propp, L. Taylor, and L. Walling, "Status of the SSC LEB RF Cavity," in *PAC 1993*, (Washington DC, USA), pp. 824–826, 1993.

[11] R. Madrak, G. Romanov, and I. Terechkine, "Static Permeability of AL-800 Garnet Material." FNAL TD note TD-15-004, April 2015.

[12] 2nd Harmonic Cavity Group, "2nd Harmonic RF Perpendicular Biased Cavity Update (05 May 2016)." Available: https://beamdocs.fnal.gov/AD-public/DocDB/ShowDocument?docid=5152, May 2016.

[13] 2nd Harmonic Cavity Group, "2nd Harmonic RF Perpendicular Biased Cavity Update (28 Sep 2017)." Available: https://beamdocs.fnal.gov/AD-public/DocDB/ShowDocument?docid=5858, September 2017.

[14] A. Ostebee and P. Zorn, *Calculus from Graphical, Numerical, and Symbolic Points of View*. Saunders College Publishing, 1997.

Appendix A

Witness Sample Analysis Code

```
#!/usr/bin/env python
# coding: utf-8
#Python 2.7

getipython().magic(u'reset -f')
import matplotlib.pyplot as plt
import numpy as np
import math
import bisect
from distutils.dirutil import mkpath
import time
import os
from scipy.interpolate import interp1d
import csv
import pandas as pd
import string
from sympy import *
from matplotlib.patches import Rectangle
getipython().magic(u'matplotlib inline')
getipython().magic(u'pylab inline')
home = os.getcwd()
initprinting(uselatex='mathjax')

#Collect data files for processing
def findall(name,path):
    result=[]
    for root,dirs,files in os.walk(path):
        if name in files:
                result.append(os.path.join(root,name))
    return result
#Calculate B field by numerical integration
def findB2(x, y):
    meany = (y[:-1] + y.shift(-1)[:-1]) / 2
    scaledint = meany*x
    scaledint2= y[:-1]*x
    scaledint3= y.shift(-1)[:-1]*x
    cumulativeint = scaledint.cumsum(axis='index')*10000
    cumulativeint2 = scaledint2.cumsum(axis='index')*10000
    cumulativeint3 = scaledint3.cumsum(axis='index')*10000
    return cumulativeint,cumulativeint2,cumulativeint3,scaledint*10000
#interpolate y(x)
def connectthedots(x,y):
    z = len(x)-1
```

```
    f = interp1d(x,y)
    xmin=round(x.min()+1)
    xmax=round(x.max()-1)
    xnew = np.arange(xmin,xmax, 1)
    ynew = f(xnew)
    return xnew,ynew
#Detect Outliers
def detectoutlier(data1):
    threshold=3
    mean1 = np.mean(data1)
    std1 =np.std(data1)
    for y in data1:
        zscore= (y - mean1)/std1
        if np.abs(zscore) ¿ threshold:
            outliers.append(y)
    return outliers
#Calculate Weighted mean and StdErr of Lot
def LotAverage(Frame,List):
    Runspersample=[]
    for sample in List:
        Runspersample.append(len(list(Frame.filter(regex=sample+' ').filter(
                                                    regex='SR'))))
    weighted=pd.DataFrame(columns=List)
    for sample,runs in zip(List,Runspersample):
        weighted[sample]=comparetable[sample+' Avg']*runs/sum(Runspersample)
    weighted['Weighted']=weighted.sum(axis=1)
    Frame['Weighted Avg']=weighted['Weighted']
    #Calculate standard error of lot
    squaredsum=pd.DataFrame()
    temp5=pd.DataFrame()
    n=len(List)
    for sample in List:
        squaredsum[sample] = (Frame['Weighted Avg']-Frame[sample+' Avg'])**2
        Frame['Weighted StdErr']= sqrt(squaredsum.sum(axis=1)/(n-1))

#input physical measurement parameters such as coil turns, resistance, sample
                                        and coil dimensions
parameters=pd.readcsv('Files"parameters.csv', sep=',',header=None)
parms = pd.tonumeric(parameters[1],errors='coerce')
meas = pd.readcsv('Files"witnessmeasurements.csv',indexcol=0)
lots = pd.readcsv('Files"witnesssamplelots.csv')
#Measured variables and uncertainties:
Lc=0.01816 #solenoid length
R=float(parameters[1][3])
dc=0.01834 #coil diameter
dV=0.000001 # Scope Voltage Precision
dLc=0.0008 # Excitation Coil Length Precision
ddc=0.00003  # Coil Diameter Precision
dL=0.0001  #Sample length precision
dR=0.01    # Primary Resistor Precision
pulsestartall=71 #Measurement pulse starts on this element in the data files
saveprefix='final2'

#Find all the excitation coil data files and calculate H and the B air gap error
                                        and the uncertainty for both for all
                                       samples
vrplist= findall('vrp.csv',home)
```

```
vrpdf = pd.DataFrame()

samplerunlist=[]
samplelist=[]
i=0
for item in vrplist:
    a=pd.DataFrame()
    b=pd.DataFrame()
    c=pd.DataFrame()
    drive, pathandfile = os.path.splitdrive(item)
    path, file = os.path.split(pathandfile)
    folders=[]
    while 1:
        path, folder = os.path.split(path)
        if folder !="":
            folders.append(folder)
        else:
            if path != "":
                folders.append(path)
            break
    folders.reverse()
    run=len(folders)-1
    sample=run-1
    #Create sample/run name from file path
    samplerun = "".join((folders[sample]," ",folders[run]," SR"))
    #Create list of sample runs:
    samplerunlist.append(samplerun)
    #Create list of samples:
    samplelist.append(folders[sample])
    #Load data from sample run:
    temp  = pd.readcsv(item,sep=',',header=None,usecols=[3,4])
    #rename data columns:
    temp.columns=[samplerun + ' T',samplerun + ' Vrp']
    #subtract the mean offset from data set:
    temp[samplerun+' Vrp']=temp[samplerun + ' Vrp']-temp[samplerun + ' Vrp'][
                                        :pulsestartall].mean(axis=0)
    H=pd.DataFrame()
    gap=pd.DataFrame()
    dH=pd.DataFrame()
    dgap=pd.DataFrame()
    temp2=pd.DataFrame()
    #Calculate H:
    L=meas[folders[sample]][0]
    N=parms[0]/Lc*L
    print meas[folders[sample]],L
    Hconverter= lambda x: x*N/(R*L)*parms[5]
    H[samplerun + ' H']= temp[samplerun + ' Vrp'].apply(Hconverter)
    #Calculate H error:
    dHconverter = lambda x: N*parms[5]*(((N*parms[5]/(L*R))**2)*(2*dV**2)*(1+
                                        1/pulsestartall)+(x*dR/R)**2+(x*
                                        dLc/Lc)**2)**(0.5)
    dH[samplerun +' dH']=H[samplerun + ' H'].apply(dHconverter)
    #Calculate gap correction of B based on sample size:
    ds=float(meas[folders[sample]]['Diameter'])
    gapconverter= lambda x: x*((dc**2)/(ds**2)-1)
    gap[samplerun + ' gap']= H[samplerun + ' H'].apply(gapconverter)
    temp2 = pd.concat([H,gap,dH], ignoreindex=False, axis=1)
```

```
    #Calculate gap error:
    temp2=temp2.assign(dgap= temp2[samplerun + ' gap']*((temp2[samplerun +'
                                            dH']/temp2[samplerun + ' H'])**2+(
                                            dc**4/(dc**2-ds**2)**2*((2*ddc/dc)
                                            **2+(2*dds/ds)**2)))**(0.5)).abs()
    temp2.rename(columns={'dgap':samplerun+' dgap' ,inplace=True)
    vrpdf    = pd.concat([vrpdf,temp,temp2], ignoreindex=False, axis=1)
#Remove duplicates from sample list:
samplelist=list(dict.fromkeys(samplelist))

#Find all measurement coil data files and calculate B
vslist = findall('vs.csv',home)
cols = []
vsdf = pd.DataFrame()
deltats = pd.DataFrame()
for item in vslist:
    a2=pd.DataFrame()
    b2=pd.DataFrame()
    c2=pd.DataFrame()
    drive, pathandfile = os.path.splitdrive(item)
    path, file = os.path.split(pathandfile)
    folders=[]
    while 1:
        path, folder = os.path.split(path)

        if folder !="":
            folders.append(folder)
        else:
            if path != "":
                folders.append(path)
            break
    folders.reverse()
    run=len(folders)-1
    sample=run-1
    #Create sample/run name from file path
    samplerun = "".join((folders[sample]," ",folders[run]," SR"))
    temp  = pd.readcsv(item,sep=',',header=None,usecols=[3,4])
    temp.columns=[samplerun + ' T',samplerun + ' Vs']
    #subtract the mean offset from data set:
    temp[samplerun+' Vs'] = temp[samplerun + ' Vs']-temp[samplerun + ' Vs'][:
                                            pulsestartall].mean(axis=0)
    #Create list of delta T for each run
    delt = temp[samplerun + ' T'][1]-temp[samplerun + ' T'][0]
    deltats[samplerun]=[delt]
    dBtemp = pd.DataFrame()
    B= pd.DataFrame()
    Bmin= pd.DataFrame()
    Bmax= pd.DataFrame()
    S= pd.DataFrame()
    #Calculate dB from Vs:
    dBconverter=lambda x: -x/(parms[1]*meas[folders[sample]]['Area'])
    dBtemp[samplerun +' dB'] = temp[samplerun + ' Vs'].apply(dBconverter)
    #Calculate B from dB:
    B[samplerun +' B'],Bmin[samplerun +' Bmin'],Bmax[samplerun +' Bmax'],
                                            S[samplerun +' Slice'] = findB2(
                                            delt,dBtemp[samplerun +' dB'])
```

```
    vsdf    = pd.concat([vsdf,temp,dBtemp,B,Bmin,Bmax,S], ignoreindex=
                                            False, axis=1)

#Calculate Bc and Mu
vsdfnoT=vsdf.drop(list(vsdf.filter(regex=' T')),axis = 1)
df   = pd.concat([vrpdf,vsdfnoT], ignoreindex=False, axis=1)
df= df.sortindex(axis=1)
for srun in samplerunlist:
    df[srun +' Bc']=df[srun +' B']-df[srun +' gap']
    df[srun +' Mu']=df[srun +' Bc']/df[srun+' H']
df.sortindex(axis=1,inplace=True)

#Calculate S for Bfield corrected calculation
tempslice=pd.DataFrame()
for srun in samplerunlist:
    tempslice[srun]=(df[srun+' Slice']*2*dds/ds)**2+(1.42*dV*2*parms[6]*
                                            deltats[srun][0]/(parms[1]*math.pi
                                            *ds**2))**2
    #df[srun+' dBn']=df[srun+' Slice']**2
tempslice=tempslice.cumsum()

#Calculate Bfieldcorrected error
dBc = pd.DataFrame()
for srun in samplerunlist:
    dBc[srun+' dBc'] = sqrt(tempslice[srun]**2+df[srun+' dgap']**2)
df   = pd.concat([df,dBc], ignoreindex=False, axis=1)

#Calculate Trapezoid Error Bound
A=-parms[6]/(parms[1]*math.pi*ds**2)
dbpprime=pd.DataFrame()
Et=pd.DataFrame()
for srun in samplerunlist:
    dbpprime[srun]=(df[srun+' dB'].shift(-1)-2*df[srun+' dB']+df[srun+' dB'
                                            ].shift(1))/deltats[srun][0]
    Et[srun+' dTrap EB'] = [dbpprime[srun].max()*2.6667e-15]
df   = pd.concat([df,Et], ignoreindex=False, axis=1)
df.sortindex(axis=1,inplace=True)

#Calculate dMu:  This calculation leaves out the trapezoid error bound which is
                                        many orders of magnitude smaller.
dMu= pd.DataFrame()
for srun in samplerunlist:
    dMu[srun+' dMu']=df[srun+' Mu'].abs()*sqrt((df[srun+' dBc']/df[srun+'
                                            Bc'])**2+(df[srun+' dH']/df[srun
                                            +' H'])**2)
df= pd.concat([df,dMu], ignoreindex=False, axis=1)

#Select data from df above Bc threshold for region of interest:
valuetofind=475
indexlist=[]
Bc=df.filter(regex='Bc')
for srun in samplerunlist:
    a= Bc.index[Bc[srun + ' Bc']¿=valuetofind].tolist()
    indexlist.append(a[0])
minrow=min(indexlist)  #minimum row that includes all data above threshold
slice1= df.iloc[minrow:498]
slice1.resetindex(drop=True,inplace=True)
```

```
#Interpolate Mu(Bc):
dfinterp=pd.DataFrame()
for srun in samplerunlist:
    x =slice1[srun+' Bc'][:slice1[srun+' Bc'].idxmax()+1].values
    y = slice1[srun+' Mu'][:slice1[srun+' Bc'].idxmax()+1].values
    xinterp,yinterp=connectthedots(x,y)
    data = pd.DataFrame( -srun+' Bci':xinterp,
                         srun+' Mui':yinterp
                           )
    dfinterp=dfinterp.merge(data,leftindex = True, rightindex = True, how =
                                          'outer')


lowerbound=max(dfinterp.filter(regex='Bci').min(axis=0))
upperbound=min(dfinterp.filter(regex='Bci').max(axis=0))

#Align Mu data to same Bci:
columnnames = ['Bci'] + samplerunlist
comparetable=pd.DataFrame()
b=arange(lowerbound,upperbound+1,1)
comparetable=pd.DataFrame(columns=columnnames)
comparetable['Bci']=b
temp=pd.DataFrame()
for srun in samplerunlist:
    aaa=srun+' Bci'
    bbb=srun+' Mui'
    newdf = dfinterp[[aaa,bbb]]
    temp=newdf.loc[(newdf[aaa]¿=lowerbound)&(newdf[aaa]¡=upperbound)]
    mu=temp[bbb].values
    comparetable[srun]=mu

#reject outliers¿¿than 3 st devs, remove from compare table and sample run list
rejectoutliers=1
if rejectoutliers==1:
    runs =comparetable.filter(regex='SR').loc[262,:].values
    outliers=[]
    outliers=detectoutlier(runs)
    names=[]
    cols=[]
    for column,name in zip(comparetable.filter(regex='SR').loc[262,:],
                                          comparetable.filter(regex='SR').
                                          columns):
        for out in outliers:
            if out== column:
                print name,column
                names.append(name)
                cols.append(column)
    comparetable.drop(columns=names,inplace=True)
    samplerunlist=[name for name in samplerunlist if name not in names]

#Calculate mean of each sample at each B
for sample in samplelist:
    comparetable[sample+' Avg']=comparetable.filter(regex=sample+' ').mean(
                                          axis=1)

#Calculate standard error of each sample mean at each B
```

```
for sample in samplelist:
    squaredsum=pd.DataFrame()
    n=0
    #print sample
    for srun in samplerunlist:
        if sample in srun:
            squaredsum[srun] = (comparetable[sample+' Avg']-comparetable[
                                                    srun])**2
            n=n+1
            #print srun
    comparetable[sample+' StdErr']= sqrt(squaredsum.sum(axis=1)/(n-1))

comparetable.sortindex(axis=1,inplace=True)

#calculate weighted sample mean of all samples
Runspersample=[]
for sample in samplelist:
    Runspersample.append(len(list(comparetable.filter(regex=sample+' ').
                                        filter(regex='SR'))))
sum(Runspersample)
weighted=pd.DataFrame(columns=samplelist)
for sample,runs in zip(samplelist,Runspersample):
    weighted[sample]=comparetable[sample+' Avg']*runs/sum(Runspersample)
weighted['Weighted']=weighted.sum(axis=1)
comparetable['Weighted Avg']=weighted['Weighted']

#Calculate mean of all samples
comparetable['All Avg']=comparetable.filter(regex=' Avg').mean(axis=1)
squaredsum=pd.DataFrame()
n=len(samplelist)
for sample in samplelist:
    squaredsum[sample] = (comparetable['All Avg']-comparetable[sample+' Avg']
                                        )**2
    comparetable['All StdErr']= sqrt(squaredsum.sum(axis=1)/(n-1))
for sample in samplelist:
    squaredsum[sample] = (comparetable['Weighted Avg']-comparetable[sample+'
                                        Avg'])**2
    comparetable['Weighted StdErr']= sqrt(squaredsum.sum(axis=1)/(n-1))
for sample in samplelist:
    comparetable[sample + ' %Diff All'] = 100*(comparetable[sample + ' Avg']-
                                        comparetable['All Avg'])/
                                        comparetable['All Avg']
    comparetable[sample + ' %Diff All'] = comparetable[sample + ' %Diff All']
for sample in samplelist:
    comparetable[sample + ' Weighted %Diff All'] = 100*(comparetable[sample +
                                        ' Avg']-comparetable['Weighted Avg'
                                        ])/comparetable['Weighted Avg']
    comparetable[sample + ' Weighted %Diff All'] = comparetable[sample + '
                                        Weighted %Diff All']

#Organize results into sample lots
sampleavglist=comparetable.filter(regex='Avg').drop('All Avg',axis=1).columns
                                    .tolist()
lotlist = lots.columns.tolist()
lot1 = lots[lotlist[0]].dropna().tolist()
lot2 = lots[lotlist[1]].dropna().tolist()
lot3 = lots[lotlist[2]].dropna().tolist()
```

```
lot4 = lots[lotlist[3]].dropna().tolist()
lot5 = lots[lotlist[4]].dropna().tolist()

temp4=pd.DataFrame(-'Bci':comparetable['Bci'] )
comparelot1=pd.DataFrame(-'Bci':comparetable['Bci'] )
comparelot2=pd.DataFrame(-'Bci':comparetable['Bci'] )
comparelot3=pd.DataFrame(-'Bci':comparetable['Bci'] )
comparelot4=pd.DataFrame(-'Bci':comparetable['Bci'] )
comparelot5=pd.DataFrame(-'Bci':comparetable['Bci'] )

for sample in lot1:
    sample=str(sample)+' '
    temp4=comparetable.loc[:,comparetable.columns.str.contains(str(sample))]
    comparelot1 = pd.concat([comparelot1,temp4], ignoreindex=False, axis=1)
for sample in lot2:
    sample=str(sample)+' '
    temp4=comparetable.loc[:,comparetable.columns.str.contains(str(sample))]
    comparelot2 = pd.concat([comparelot2,temp4], ignoreindex=False, axis=1)
for sample in lot3:
    sample=str(sample)+' '
    temp4=comparetable.loc[:,comparetable.columns.str.contains(str(sample))]
    comparelot3 = pd.concat([comparelot3,temp4], ignoreindex=False, axis=1)
for sample in lot4:
    sample=str(sample)+' '
    temp4=comparetable.loc[:,comparetable.columns.str.contains(str(sample))]
    comparelot4 = pd.concat([comparelot4,temp4], ignoreindex=False, axis=1)
for sample in lot5:
    sample=str(sample)+' '
    temp4=comparetable.loc[:,comparetable.columns.str.contains(str(sample))]
    comparelot5 = pd.concat([comparelot5,temp4], ignoreindex=False, axis=1)

#Calculate weighted mean and Std of all lots
LotAverage(comparelot1,lot1)
LotAverage(comparelot2,lot2)
LotAverage(comparelot3,lot3)
LotAverage(comparelot4,lot4)
LotAverage(comparelot5,lot5)

#Calculate mean and Std of all lot 1
comparelot1['Lot1 Avg']=comparelot1.filter(regex=' Avg').mean(axis=1)
squaredsum=pd.DataFrame()
temp5=pd.DataFrame()
n=len(lot1)
for sample in lot1:
    squaredsum[sample] = (comparelot1['Lot1 Avg']-comparelot1[sample+' Avg
                                                    '])**2
    comparelot1['Lot1 StdErr']= sqrt(squaredsum.sum(axis=1)/(n-1))
#Calculate mean of all lot 2
comparelot2['Lot2 Avg']=comparelot2.filter(regex=' Avg').mean(axis=1)
squaredsum=pd.DataFrame()
temp5=pd.DataFrame()
n=len(lot2)
for sample in lot2:
    squaredsum[sample] = (comparelot2['Lot2 Avg']-comparelot2[sample+' Avg
                                                    '])**2
    comparelot2['Lot2 StdErr']= sqrt(squaredsum.sum(axis=1)/(n-1))
#Calculate mean of all lot 3
```

```
comparelot3['Lot3 Avg']=comparelot3.filter(regex=' Avg').mean(axis=1)
squaredsum=pd.DataFrame()
temp5=pd.DataFrame()
n=len(lot3)
for sample in lot3:
    squaredsum[sample] = (comparelot3['Lot3 Avg']-comparelot3[sample+' Avg
                                                    '])**2
    comparelot3['Lot3 StdErr']= sqrt(squaredsum.sum(axis=1)/(n-1))
#Calculate mean of all lot 4
comparelot4['Lot4 Avg']=comparelot4.filter(regex=' Avg').mean(axis=1)
squaredsum=pd.DataFrame()
temp5=pd.DataFrame()
n=len(lot4)
for sample in lot4:
    squaredsum[sample] = (comparelot4['Lot4 Avg']-comparelot4[sample+' Avg
                                                    '])**2
    comparelot4['Lot4 StdErr']= sqrt(squaredsum.sum(axis=1)/(n-1))
#Calculate mean of all lot 5
comparelot5['Lot5 Avg']=comparelot5.filter(regex=' Avg').mean(axis=1)
squaredsum=pd.DataFrame()
temp5=pd.DataFrame()
n=len(lot5)
for sample in lot5:
    squaredsum[sample] = (comparelot5['Lot5 Avg']-comparelot5[sample+' Avg
                                                    '])**2
    comparelot5['Lot5 StdErr']= sqrt(squaredsum.sum(axis=1)/(n-1))

#Save results
df.tocsv(saveprefix+'df.csv')
comparetable.tocsv(saveprefix+'comparetable.csv')
comparelot1.tocsv(saveprefix+'comparelot1.csv')
comparelot2.tocsv(saveprefix+'comparelot2.csv')
comparelot3.tocsv(saveprefix+'comparelot3.csv')
comparelot4.tocsv(saveprefix+'comparelot4.csv')
comparelot5.tocsv(saveprefix+'comparelot5.csv')
```

Appendix B

Witness Sample Systematic Error Propagation

B.1 Error Propagation Rules

The purpose of this section is to determine accurate error estimates for ΔB,ΔH, and $\Delta\mu$, for the calculation of B, H, and μ, where

$$\mu = \frac{B}{H} \tag{B.1.1}$$

$$\Delta\mu = |\mu|\sqrt{\frac{\Delta B^2}{B^2} + \frac{\Delta H^2}{H^2}} \tag{B.1.2}$$

Errors are propagated using the following rules, assuming all the variables on the right-hand side are independent:

a)	$R = X + Y + Z$	$\Delta R = \sqrt{\Delta X^2 + \Delta Y^2 + \Delta Z^2}$
b)	$R = \frac{XY}{Z}$	$\Delta R = \lvert R\rvert\sqrt{\frac{\Delta X^2}{X^2} + \frac{\Delta Y^2}{Y^2} + \frac{\Delta Z^2}{Z^2}}$
c)	$R = cX$	$\Delta R = \lvert c\rvert\Delta X$
d)	$R = X^n$	$\Delta R = \lvert n\rvert\frac{\Delta X}{\lvert X\rvert}\lvert R\rvert$

The calculation of μ is done in several steps and includes six measured variables. ΔB and ΔH can be calculated separately and then combined to find $\Delta\mu$ using equation B.1.2.

B.2 Error Calculation of the H field

$$H = \frac{N_e V_{rp} f}{LR} \tag{B.2.1}$$

Starting with the equation for H above from equation 2.5.1, and including a scaling factor f for cgs units, the measured variables are V_{rp}, L, and R. L is the length of the coil, R is the resistance of the shunt resistor, and N_e is the number of windings in the excitation coil. ΔL and ΔR are easily found from the uncertainty of the measuring devices. V_{rp} represents the voltage across the shunt resistor. It is determined by finding the difference V_H of the measured voltage to ground on either side of the shunt resistor and then subtracting the DC offset F_H.

$$V_{rp} = V_H - F_H \tag{B.2.2}$$

$$V_H = V_1 - V_2 \tag{B.2.3}$$

$$F_H = \sum_i^m \frac{V_{Hi}}{m} \tag{B.2.4}$$

F_H is found by finding the average V_H in the flat pre-pulse region using equation B.2.4, where m is the number of points averaged for the offset correction.

The voltage uncertainty of the oscilloscope is given by ΔV. Applying the propagation rules to the above equations yields ΔV_H and ΔF_H.

$$\Delta V_1 = \Delta V_2 = \Delta V \tag{B.2.5}$$

$$\Delta V_H = \sqrt{\Delta V_1^2 + \Delta V_2^2} = \sqrt{2}\Delta V \tag{B.2.6}$$

$$\Delta F_H = \frac{1}{m}\sqrt{\sum_i^m \Delta V_{Hi}^2} = \frac{1}{m}\sqrt{\sum_i^m 2\Delta V_i^2} = \frac{\sqrt{2}\Delta V}{\sqrt{m}} \tag{B.2.7}$$

$$\Delta V_{rp} = \sqrt{2\Delta V^2 + \frac{2\Delta V^2}{m}} \tag{B.2.8}$$

ΔH can be calculated in terms of the measured H, R, L and the fundamental measurement uncertainties using rules b) and c).

$$\Delta H = |H| N_e f \sqrt{\frac{\Delta V_{rp}^2}{V_{rp}^2} + \frac{\Delta R^2}{R^2} + \frac{\Delta L^2}{L^2}} \tag{B.2.9}$$

$$\Delta H = N_e f \sqrt{\frac{H^2 \Delta V_{rp}^2}{V_{rp}^2} + \frac{H^2 \Delta R^2}{R^2} + \frac{H^2 \Delta L^2}{L^2}} \tag{B.2.10}$$

$$\boxed{\Delta H^2 = N_e^2 f^2 \left[\left(\frac{N_e f}{LR} \right)^2 \left(2\Delta V^2 + \frac{2\Delta V^2}{m} \right) + H^2 \left(\frac{\Delta R^2}{R^2} + \frac{\Delta L^2}{L^2} \right) \right]} \tag{B.2.11}$$

B.3 Error Calculation of the B field

The derivation of ΔB is somewhat more complicated than the derivation of ΔH. The expression for B without the air gap correction is given below in B.3.1, which is the first term in equation 2.5.8. G is a scaling factor, t is the time interval between data points, V_s is the voltage reading on the measurement coil that has been corrected for the oscilloscope internal offset, N_m is the number of windings on the measurement coil, and d_s is the sample diameter.

$$B_n = -\sum_i^n \frac{2Gt\,(V_{si} + V_{si+1})}{N_m \pi d_s^2} \tag{B.3.1}$$

Let A be the constants and X_i be the summation terms.

$$B_n = -\sum_i^n AX_i \tag{B.3.2}$$

Then S is a single area element j of the integration sum.

$$S_j = AX_j \tag{B.3.3}$$

$$A = \frac{2Gt}{N_m \pi d_s^2} \tag{B.3.4}$$

$$X_j = \left(V_{sj} + V_{sj+1}\right) \tag{B.3.5}$$

Then, using rule b), the error on a single integration area element can be found.

$$\Delta S_j = S_j \sqrt{\left(\frac{\Delta A}{A}\right)^2 + \left(\frac{\Delta X_j}{X_j}\right)^2} = \sqrt{\left(\frac{\Delta A S_j}{A}\right)^2 + \left(\Delta X_j A\right)^2} \tag{B.3.6}$$

The error ΔB_n of the integrated area from 0 to n can be calculated from ΔS_j.

$$\Delta B_n = \sqrt{\sum_j^n \Delta S_j^2} \tag{B.3.7}$$

To find ΔS, ΔA and ΔX_j must be found. From B.3.4,

$$A = \frac{2Gt}{N_m \pi} d_s^{-2} = C d_s^{-2} \tag{B.3.8}$$

and using rule d),

$$\Delta A = |2| \frac{\Delta d_s}{|d_s|} \left|C d_s^{-2}\right| = 2C d_s^{-3} \Delta d_s = 2A d_s^{-1} \Delta d_s \tag{B.3.9}$$

$$\frac{\Delta A}{A} = 2\frac{\Delta d_s}{d_s} \tag{B.3.10}$$

V_s is the voltage from the measurement coil, V_B, which has been corrected for the offset by F_B.

$$\Delta X_j = \sqrt{\Delta V_{sj}^2 + \Delta V_{sj+1}^2} = \sqrt{2}\Delta V_s \tag{B.3.11}$$

$$V_s = V_B + F_B \tag{B.3.12}$$

As done in equations B.2.4 and B.2.7,

$$\Delta F_B = \frac{\Delta V}{\sqrt{m}} \tag{B.3.13}$$

$$\Delta V_B = \Delta V \tag{B.3.14}$$

$$\Delta V_s = \sqrt{\Delta V_B^2 + \Delta F_B^2} = \sqrt{\Delta V^2 + \frac{\Delta V^2}{m}} = \Delta V \sqrt{1 + \frac{1}{m}} \tag{B.3.15}$$

ΔX_j can be found by combining equations B.3.11 and B.3.15 and letting $m = 71$.

$$\Delta X_j = 1.42 \Delta V \tag{B.3.16}$$

ΔB_n is found by substituting equations B.3.10 and B.3.16 into B.3.6, and then applying rule a) to the integrated sum.

$$\Delta S_j = S_j \sqrt{\left(\frac{\Delta A}{A}\right)^2 + \left(\frac{\Delta X_j}{X_j}\right)^2} = \sqrt{\left(\frac{\Delta A S_j}{A}\right)^2 + \left(\Delta X_j A\right)^2} \tag{B.3.17}$$

$$\Delta S_j = \sqrt{\left(2\frac{\Delta d_s S_j}{d_s}\right)^2 + \left(1.42 \Delta V \frac{2Gt}{N_m \pi d_s^2}\right)^2} \tag{B.3.18}$$

$$\boxed{\Delta B_n = \sqrt{\sum_i^n \left(2\frac{\Delta d_s S_i}{d_s}\right)^2 + \left(1.42 \Delta V \frac{2Gt}{N_m \pi d_s^2}\right)^2}} \tag{B.3.19}$$

B.4 Error Calculation of the B Field Air Gap Calculation

The B field calculation also includes a correction for the air gap, g, between the sample and the measurement coil that is dependent on H and the measured diameters of the coil and sample. The B field in the air gap is equal to the H field in cgs units multiplied by the ratio of air gap area to garnet area. The ratio of air gap area to garnet area reduces to the ratio of the difference between the squares of the diameters of the sample and coil. In the equations below, d_s and d_c are the sample diameter and measurement coil diameter. Returning to equation 2.5.8 in cgs units and including the above mentioned terms:

$$B_{\text{garnet}} = \left[-\sum_i^n \frac{2Gt\,(V_{Bi} + V_{Bi+1})}{N_m \pi d_s^2} \right] - g_n \tag{B.4.1}$$

$$g_n = \frac{H_n}{d_s^2}\left(d_c^2 - d_s^2\right) = H_n \left(\frac{d_c^2}{d_s^2} - 1\right) = H_n M \tag{B.4.2}$$

$$\Delta g_n = |H_n M| \sqrt{\left(\frac{\Delta H_n}{H_n}\right)^2 + \left(\frac{\Delta M}{M}\right)^2} \tag{B.4.3}$$

$$M = \frac{d_c^2}{d_s^2} - 1 = \alpha\gamma - 1 \tag{B.4.4}$$

$$\Delta M = \Delta\left(\alpha\gamma\right) \tag{B.4.5}$$

$$\Delta M = |\alpha\gamma| \sqrt{\left(\frac{\Delta\alpha}{\alpha}\right)^2 + \left(\frac{\Delta\gamma}{\gamma}\right)^2} \tag{B.4.6}$$

$$\alpha = d_c^2 \qquad\qquad \gamma = d_s^{-2}$$

$$\Delta\alpha = \frac{|2|\,\Delta d_c d_c^2}{|d_c|} = 2d_c\Delta d_c \tag{B.4.7}$$

$$\Delta\gamma = \frac{|-2|\,\Delta d_s d_s^{-2}}{|d_s|} = 2d_s^{-3}\Delta d_s \tag{B.4.8}$$

$$\Delta M = \frac{d_c^2}{d_s^2}\sqrt{\left(\frac{2d_c\Delta d_c}{d_c^2}\right)^2 + \left(\frac{2d_s^{-3}\Delta d_s}{d_s^{-2}}\right)^2} = \frac{d_c^2}{d_s^2}\sqrt{\left(\frac{2\Delta d_c}{d_c}\right)^2 + \left(\frac{2\Delta d_s}{d_s}\right)^2} \tag{B.4.9}$$

$$\Delta g_n = |g_n| \sqrt{\left(\frac{\Delta H_n}{H_n}\right)^2 + \left(\frac{\frac{d_c^2}{d_s^2}\sqrt{\left(\frac{2\Delta d_c}{d_c}\right)^2 + \left(\frac{2\Delta d_s}{d_s}\right)^2}}{\frac{d_c^2}{d_s^2} - 1}\right)^2} \tag{B.4.10}$$

$$\Delta g_n = |g_n| \sqrt{\left(\frac{\Delta H_n}{H_n}\right)^2 + \frac{d_c^4}{\left(d_c^2 - d_s^2\right)^2}\left(\left(\frac{2\Delta d_c}{d_c}\right)^2 + \left(\frac{2\Delta d_s}{d_s}\right)^2\right)} \tag{B.4.11}$$

Equations B.3.19 and B.4.11 are combine using rule a) to obtain the error for the calculated B field with the air gap correction.

$$\boxed{\begin{aligned}\Delta B_{\text{garnet}}^2 = &\left[\sum_i^n \left(2\frac{\Delta d_s S_i}{d_s}\right)^2 + \left(1.42\Delta V \frac{2Gt}{N_m \pi d_s^2}\right)^2\right] \\ &+ g_n^2\left[\left(\frac{\Delta H_n}{H_n}\right)^2 + \frac{d_c^4}{\left(d_c^2 - d_s^2\right)^2}\left(\left(\frac{2\Delta d_c}{d_c}\right)^2 + \left(\frac{2\Delta d_s}{d_s}\right)^2\right)\right]\end{aligned}} \tag{B.4.12}$$

B.5 Numerical Integration Trapezoidal Rule Error Bound

The last component of error in the B calculation is the error due to using a trapezoidal method numerical integration. In the witness sample calculations, the magnitude of the trapezoidal rule error bound is several orders of magnitude smaller than the error from all other sources and is assumed to be zero in the calculations. The analysis is included here only for completeness.

The error bound, E, for an approximation of the numerical integration of a function $f(x)$ can be determined by the following expression [14]:

$$|E| \leq \frac{K\,(b-a)^3}{12n^2} \text{ if } K \geq |f''(x)| \text{ for all } x \text{ in } [a,b] \tag{B.5.1}$$

where $[a,b]$ is the interval being integrated and n is the number of sub-intervals.

The second derivative of $f(x)$ can be determined by using the numerical finite difference approximation where h is the time interval t_Δ between data points:

$$f''\left(x_j\right) = \frac{f\left(x_{j+1}\right) - 2f\left(x_j\right) + f\left(x_{j-1}\right)}{h} \tag{B.5.2}$$

Applying B.5.2 to equation B.3.1,

$$B_n(t) = -\sum_i^n \frac{2Gt_\Delta\left(V_i(t) + V_{i+1}(t)\right)}{N_m \pi d_s^2} \tag{B.5.3}$$

$$\left|B''(t_j)\right| = \left|-\frac{G}{N_m \pi d_s^2}\left(V(t_{j+1}) - 2V(t_j) + V(t_{j-1})\right)\right| \tag{B.5.4}$$

If K equals the maximum value of $B''(t)$, while $(b-a) = 0.002$, and $n = 500$, then the error bound can be found using equation B.5.1.

$$|E| \leq \frac{B''(t_{max})0.002^3}{12 \cdot 500^2} \tag{B.5.5}$$

$$\boxed{|E| \leq 2.667 \cdot 10^{-15} B''(t_{max})} \tag{B.5.6}$$

As can be seen in equation B.5.6, the trapezoidal error bound in the B field calculation will be very small, except in the case of extremely large $B''(t)$. In the case of the witness sample calculations, this component of the error is assumed to be zero.

B.6 Error Calculation of μ

Returning to equation B.1.2, the systematic error of the calculation of μ can be found by substituting in the expressions for ΔH and ΔB from equations B.2.11 and B.4.12.

$$\Delta\mu^2 = \mu^2\left(\frac{\Delta B^2}{B^2} + \frac{\Delta H^2}{H^2}\right) \tag{B.6.1}$$

$$
\begin{aligned}
\Delta\mu_n^2 = {} & \frac{\mu_n^2}{B_n^2}\left[\sum_i^n\left(2\frac{\Delta d_s S_i}{d_s}\right)^2+\left(1.42\Delta V\frac{2Gt}{N_m\pi d_s^2}\right)^2\right] \\
& +\frac{\mu_n^2 g_n^2 N_e^2 f^2}{B_n^2 H_n^2}\left[\left(\frac{N_e f}{LR}\right)^2\left(2\Delta V^2+\frac{2\Delta V^2}{m}\right)+H^2\left(\frac{\Delta R^2}{R^2}+\frac{\Delta L^2}{L^2}\right)\right] \\
& +\frac{\mu_n^2 g_n^2 d_c^4}{B_n^2\left(d_c^2-d_s^2\right)^2}\left[\left(\frac{2\Delta d_c}{d_c}\right)^2+\left(\frac{2\Delta d_s}{d_s}\right)^2\right] \\
& +\frac{\mu_n^2 N_e^2 f^2}{H_n^2}\left[\left(\frac{N_e f}{LR}\right)^2\left(2\Delta V^2+\frac{2\Delta V^2}{m}\right)+H_n^2\left(\frac{\Delta R^2}{R^2}+\frac{\Delta L^2}{L^2}\right)\right]
\end{aligned}
\tag{B.6.2}
$$